A Scalable Energy vs Latency Trade-off in Full Duplex Mobile Edge Computing Systems

Mahmoud T. Kabir, *Student Member, IEEE,* and Christos Masouros, *Senior Member, IEEE*

***Abstract*—In this paper, we investigate the offloading energy and latency trade-off in a multiuser full-duplex (FD) system. We consider a multi-user FD system where a FD base station (BS), equipped with a mobile-edge computing (MEC) server, carries out data transmission in the downlink, while at the same time receiving computational tasks from mobile devices in the uplink. Our main aim is to study the trade-off between the offloading energy and latency, which are known to be very important and desirable system objectives for both the system operator and users. In practice, there always exist a trade-off between these two objectives. Towards this aim, we formulate two weighted multi-objective optimization problems (MOOPs), one, where the multi-user interference (MUI) is suppressed and the other, where MUI is rather exploited. As a result, our proposed MOOPs allow for a scalable tradeoff between the two objectives. To tackle the non-convexity of the formulations, we design an iterative algorithm through Lagrangian method. We also, address the scenario of imperfect channel state information (CSI) at the FD BS. For the imperfect CSI case, we apply convex relaxations and transformation using the S-procedure to tackle the non-convexity of the formulations. Simulation results show the effectiveness of the proposed FD schemes compared with the existing baseline half duplex schemes, and the superiority of MUI exploitation over suppression.**

***Index Terms*—Full-duplex, MEC, multi-objective optimization, offloading, energy, latency, interference suppression, constructive interference, robust designs.**

I. Introduction

The continuous growth of the wireless network has increased the demand for better quality of service (QoS) and reliability. The next generation 5G network aims at providing higher data rate and low latency. Full duplex (FD) has recently been brought to forefront of 5G technologies as one of the main enabler of higher data rates, since, FD allows simultaneous transmission and reception. Thanks to the major breakthroughs with regards self interference (SI) cancellation [1]–[3], various practical implementation issues such as protocols and resource allocation algorithms have been investigated. For example, [4] studied the resource allocation for distributed antenna systems with a FD base station (BS) that simultaneously serve uplink and downlink users where the network power consumption in minimized by jointly optimizing the downlink beamformer and uplink transmit power. Similarly, in [5], the authors investigated a power efficient resource allocation design for secure communications in a similar FD system setup. In addition, the trade-off between the uplink and downlink power consumption was investigated in [5], [6]. In [7], a joint design for precoding and decoding in a multi-antenna FD relay system was studied to maximize the end-to-end system performance. The spectral and energy efficiency maximization problems in a FD massive multple-input multiple-output (MIMO) relay system were studied in [8]. In contrast to the above works, which are all based on the concept of the traditional interference suppression, where, multi-user interference (MUI) is treated as unwanted, a multi-user FD system was studied in [9]–[11] by exploiting the downlink MUI rather than suppressing it. In [11], it was shown that by exploiting the downlink MUI, the downlink transmit power is reduced significantly. In addition, although the downlink MUI is exploited, the power gains extend to the uplink through the self-interference serving as the link [9]. Similarly, a robust multi-user FD design with simultaneous wireless information and power transfer (SWIPT) was investigated in [10].

On the other hand, mobile edge computing (MEC) has been identified as a promising solution to enable mobile devices (MD) offload their intensive and latency-critical computation tasks to the MEC servers for execution. In this way, the battery life at the MD can be enhanced while their data storage capabilities and computational resources can be relaxed [12]. In quest to reap the benefits of the MEC, several resource allocation designs have been proposed. [13] investigated resource allocation design for MEC systems based on time-division multiple access (TDMA) and orthogonal frequency division multiple access (OFDMA) offloading by considering the local computation capabilities of the users to minimize the mobile energy consumption. While in [14], an offline heuristic algorithm was designed to minimize the average completion time of multiple users for partitioning and scheduling the offloading of their computations. In [15], a wireless powered multiuser MEC system was proposed where the devices depend on their harvested energy to compute locally or offload tasks to the MEC server while the energy consumption of the MEC server is minimized. [16] formulated an offloading problem to minimize the energy consumption by jointly optimizing the mobile precoding matrices and the computing frequency while meeting latency constraints. Similarly, [17] proposed a game theoretic approach for computation mobile offloading in a multi-user MEC system. However, in all the above works, the authors focused on half duplex transmission and on a single-objective i.e., either energy consumption or latency objectives. In [18], the authors studied the effects of using multiple access points (APs) with computation capabilities for offloading tasks in order to minimize the energy consumption and latency for fixed and elastic central processing unit (CPU) frequency.

This work was supported in part by the Engineering and Physical Sciences Research Council Project under Grant EP/R007934/1 and in part by the Petroleum Technology Development Fund (PTDF) of the Federal Republic of Nigeria.

Mahmoud T. Kabir and C. Masouros are with the Department of Electronic and Electrical Engineering, University College London, London WC1E 7JE, U.K. (e-mail: kabir.tukur.15@ucl.ac.uk, c.masouros@ucl.ac.uk).

However, the authors assumed fixed transmitting and receiving power in their analysis, and in addition, the authors like the authors in [13]–[17], assumed that the APs have perfect channel state information (CSI). These assumptions may deviate from practical scenarios.

In the area of multi-user FD systems, only limited works have been done on mobile-edge computing (MEC). [19] studied energy harvesting with MEC, where a FD relay assists a mobile user to connect to an access point (AP) integrated with a MEC server. The user uploads part of its computation bits to the AP for execution and then, uses power splitting to download the results and harvest energy within a time frame. The paper minimizes the system energy consumption subject to latency and energy constraints by assuming perfect channel state information (CSI) with perfect self-interference (SI) cancellation at the FD relay. In [20], a similar system model is employed where users offload computation bits to a FD AP for execution and simultaneously the FD AP transmits energy to the users. The authors investigated the max-min energy efficiency problem to ensure fairness between users. Also, the authors [21], [22] investigated FD with MEC in wireless network virtualization. [21] studied the virtual resource allocation for heterogeneous services in FD-enabled small cell networks with MEC and caching while [22] proposed a MEC framework for a user virtualization scheme in the software-defined network virtualization cellular network.

Accordingly, in this paper, we study a multiuser FD MEC-supported system which comprises a FD BS equipped with a MEC server. The FD BS sends information signals in the downlink and receive intensive and latency-critical computation tasks to be executed by the MEC server through the uplink. Unlike existing works on MEC [13]–[18], we employ FD, which brings the need to optimize the variables for both uplink and downlink transmission i.e., the uplink transmit power and the downlink beamforming vectors, at the same time. However, when half duplex (HD) is employed as in [13]–[18], only the uplink or downlink variable is optimized. Also, FD introduces the self-interference (SI) signal, which is an additional term in the constraints that is non-trivial to handle as will be evident in later sections. In addition, we formulate an optimisation problem which involves minimising two desirable but conflicting system objectives, namely the total offloading energy and latency. Different to the existing works on FD [4]–[11] and MEC [13]–[22], this calls for a weighted multi-objective formulation in order to study their trade-off which is highly dependent on the optimisation variables. Thus, existing methods in [13]–[22], can not be applied to solve the proposed optimization problems directly.

Furthermore, as will be shown later, the simulation results show the performance gains achieved by the FD proposed schemes compared to the existing half-duplex (HD) schemes. We summarize our contributions below:

1) We first define the two system objectives namely, the total offloading energy and latency, then we formulate two weighted multi-objective optimization problems (MOOPs) subject to offloading latency constraints and downlink QoS constraints. One, based on interference suppression (IS) and the other, based on constructive interference (CI).
2) To solve the non-convex problems, we employ the Lagrangian method in order to design a tractable iterative algorithm for both the IS scheme and IE scheme.
3) We further extend our designs to robust formulations of the optimization problems for both IS and CI schemes by considering the worst-case performance model. To tackle the non-convexity of the formulations, we simplify and relax the constraints using auxiliary variables and then we use the S-procedure to transmform the constraints into linear matrix inequalities.

As this point we highlight some of the challenges and the practicability of the proposed FD MEC system. The implementation of FD communication systems in practice is very challenging. Although, the main challenge of FD system implementation is that of finding techniques to mitigate the performance degradation caused by SI, which has been studied in the literature thoroughly, there are other issues involved such as hardware limitations. In theory, a FD BS having large dynamic range and perfect CSI, can perfectly suppress the SI. However, in practice such is not the case, the CSI can not be perfectly estimated due to errors in pilot signals, transmission delays and mismatch, and so on, all can increase the residual SI even after cancellation and co-channel interference (CCI) in the system. For this reason, we have presented robust designs for our proposed MOOPs based on imperfect CSI with estimation error bounds in Section IV. In addition, hardware limitations such as transmit and receive signal quantization errors, nonlinearities in the system, in-phase and quadrature (I/Q) mismatch, are great challenges encountered in FD communication systems implementation that can degrade the overall performance of the system significantly. Furthermore, we emphasize the practicability of the considered FD MEC system. Particularly, in the context of ultra-dense 5G networks, each small cell BS will simultaneously serve variety of users within a small region [23], hence, each BS can be equipped with MEC servers and if the BSs operate in FD, uplink and downlink transmission can be utilized. For example, the FD BS can utilise the downlink to transmit information signals to downlink users and in the uplink, there could be a smart phone user running an intensive applications, a car or bunch of cars running real time applications such as navigation system, a wireless sensor network running latency-critical tasks like video surveillance, object tracking, e.t.c, or even an online gamer(s) interacting in real time, trying to utilise the MEC server at the FD BS.

The rest of the paper is organised as follows. In Section II, the system model of the FD based MEC system is introduced. The weighted MOOP is formulated in Section III for the case of perfect CSI and in Section IV, for the case of imperfect CSI. Section V discusses and analyses the simulation results. And, Section VI provides the concluding remarks.

II. System Model

We consider a multiuser wireless communication system as shown in Fig. 1. The system consists of a FD BS, integrated

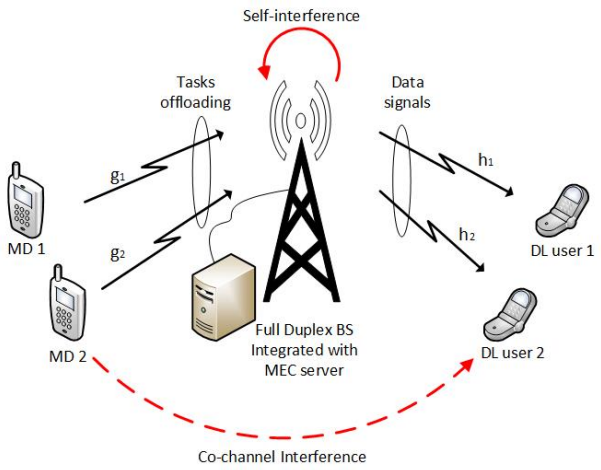

Fig. 1. A multiuser FD MEC system

with a MEC server, with N transmit and N receive antennas simultaneously serving K single-antenna downlink users and J single-antenna mobile devices. In this system, the downlink users receive information signals from the FD BS, while, the mobile devices leverage the MEC server at the FD BS to offload its latency-sensitive computation tasks, which can not be locally executed, to be executed by the MEC server. Please note that for uplink and downlink user scheduling in the resource block, we assume that this can be dealt with by existing protocols as in [13], [15].

A. Downlink Transmission

For the transmission of information signal from the FD BS to the *i-th* downlink user, let $d_i, \mathbf{h}_i \in \mathbb{C}^{N\times 1}$ and $\mathbf{w}_i \in \mathbb{C}^{N\times 1}$ be the unit data symbol, the channel vector and the beamforming vector between the FD BS and the *i-th* downlink user, respectively. Hence, the received signals at the *i-th* downlink user is given by

$$y_i = \mathbf{h}_i^H \sum_{k=1}^{K} \mathbf{w}_k d_k + \sum_{j=1}^{J} \sqrt{p_j}\ell_{j,i} + n_i, \tag{1}$$

where, p_j and $n_i \sim \mathcal{CN}\left(0, \sigma_i^2\right)$ denote the transmit power for the *j-th* mobile device and the additive white Gaussian noise at the *i-th* user, respectively. $\ell_{j,i}$ is the channel between the *j-th* mobile device and the *i-th* downlink user.

B. Computation Offloading

We denote the computation task to be offloaded to the MEC server for execution in bits at the *j-th* mobile device as q_j, which are classified as either energy consuming or time consuming tasks for the battery-constrained and time-constrained mobile device [12]. Computation offloading to the MEC server involves the transmission of the computation tasks to the FD BS by each mobile device and downloading[1] of the results by each user. Hence, we define the transmission rate of the *j-th* mobile device with bandwidth B as

$$r_j = B\log_2\left(1+\gamma_j\right), \tag{2}$$

where

$$\gamma_j = \frac{p_j\left|\mathbf{g}_j^H\mathbf{u}_j\right|^2}{\sum_{n\neq j}^{J} p_n\left|\mathbf{g}_n^H\mathbf{u}_j\right|^2 + s_j + \sigma_j^2\left\|\mathbf{u}_j\right\|^2}. \tag{3}$$

In addition, $\mathbf{g}_j \in \mathbb{C}^{N\times 1}$ denotes the channel between the FD BS and the *j-th* mobile device and σ_j^2 is the noise power at the FD BS. We denote $\mathbf{u}_j \in^{N\times 1}$ as the receive beamforming vector for the *j-th* mobile device. In this paper, to reduce complexity, we adopt zero-forcing (ZF) beamforming at the FD BS for the detection of the offloaded tasks. ZF is adopted since it provides a good trade-off between complexity and performance [24]. Hence, the receive beamforming vector for the *j-th* mobile device is given as

$$\mathbf{u}_j = (\mathbf{c}_j\mathbf{G}^\dagger)^H, \tag{4}$$

where $\mathbf{c}_j = [\underbrace{0,\ldots,0}_{j-1},1,\underbrace{0,\ldots,0}_{J-j}]$, $\mathbf{G}^\dagger = (\mathbf{G}^H\mathbf{G})^{-1}\mathbf{G}^{H,\dagger}$ denotes the pseudo-inverse operation and $\mathbf{G} = [\mathbf{g}_1,\ldots,\mathbf{g}_J]$. Furthermore, due to the simultaneous transmission and reception at the FD BS, there is a strong interference called self-interfere nce (SI) that degrades the reception of the offloaded computation tasks at the FD BS. In the literature, there are different SI mitigation techniques which could be employed to reduce the effects of SI. In order to isolate our proposed scheme from the specific implementation of any passive or active SI mitigation techniques, we model the SI after cancellation as $s_j = \sum_{i=1}^{K}\mathrm{Tr}\left\{\mathbf{w}_i\mathbf{w}_i^H\mathbf{H}_{\mathrm{SI}}^H\mathbf{u}_j\mathbf{u}_j^H\mathbf{H}_{\mathrm{SI}}\right\}$ [6], [25], where the matrix $\mathbf{H}_{\mathrm{SI}} \in \mathbb{C}^{N\times N}$ denotes the SI channel at the FD BS. Accordingly, given the computation task q_j to be offloaded by the *j-th* mobile device, the total offloading latency is defined as the time taken to offload the task q_j to the FD BS plus the time taken for the FD BS to compute the corresponding result. This can be expressed as [18]

$$T_j^{\mathrm{total}} = \underbrace{\frac{q_j}{r_j}}_{t_{off,j}} + \underbrace{\frac{q_j L_{\mathrm{BS},j}}{f_{\mathrm{BS}}}}_{t_{\mathrm{BS},j}}. \tag{5}$$

We denote $t_{off,j}$ as the time it takes to offload task q_j to the FD BS and $t_{\mathrm{BS},j}$ as the computation time at the FD BS for task q_j, where $L_{\mathrm{BS},j}$ (cycles/bit) is the number of CPU cycles required to compute 1 input bit of q_j at the FD BS and f_{BS} (cycles/s) is the CPU frequency of the FD BS. Thus, the corresponding total computation energy consumed in the offloading process by all the mobile devices is [26]

$$E_{off} = \sum_{j=1}^{J} p_j t_{off,j}. \tag{6}$$

We note here the dependency of the transmit power of the mobile devices and the downlink beamforming vectors, in that, p_j through the SI term (s_j) is a function of $\mathbf{w}_i$, which in turn is a function of p_j through (1).

[1] As the computational results are usually small, in our analysis we ignore the downloading time and the power consumed during transmitting and receiving the results [12], [15]. Thus, in this paper, our focus is particularly on the offloading of the tasks. We set aside the consideration of the results downloading from the FD BS to the mobile devices for our future work.

III. Problem Formulation

Our main objective in this paper is to study the trade-off between two important and desirable system objectives, namely, the total offloading energy and the total offloading latency. In practice, there always exist a trade-off between these two objectives, in that, on one hand, an increase in the offloading energy implies increase in transmit power of the mobile devices and in essence, leads to a decrease in the offloading latency and vice versa. In the literature, multi-objective optimization (MOO) is often employed to study the trade-off between conflicting objectives via the concept of Pareto optimality. A point is said to be Pareto optimal if there is no other point that improves any of the objectives without decreasing the others [27]. It has been shown in [27] that, one way to capture the complete Pareto optimal set of the MOOP is through the weighted-sum formulation, which can achieve the complete Pareto optimal set with low computational complexity. Thus, in order to efficiently analyse and address this trade-off between these objectives, we adopt the sum- weighted MOO that aims at minimizing the two objectives by jointly optimizing the downlink beamforming vectors and the transmit power for each mobile device, while satisfying the total offloading latency requirement constraint and downlink users QoS constraints as well as the power constraints. In the following subsections, we present two strategies for the trade-off design, one based on classical interference suppression and one based on interference exploitation.

We note that in this section, we assume that the FD BS knows all the channel state information (CSI) from and to all the users in the system. We focus on slow fading channel scenario, where the channels change at the beginning of each frame. Thus, to facilitate the channel realization in practice, handshaking is performed between the FD BS and all users. As the channel changes slowly, pilot signals are usually embedded in the data packets, which allows the FD BS to constantly update the CSI estimation of the transmission links of the users and devices. However, we explicitly treat the case of imperfect CSI in Section IV.

A. Trade-off Optimization based on Interference Suppression

First, in this section, we define the signal-to-interference plus noise ratio (SINR) at the *i-th* downlink user that promotes interference suppression (IS) transmission based on (1) as

$$\Gamma_i^{\mathrm{DL}} = \frac{|\mathbf{h}_i^H \mathbf{w}_i|^2}{\sum_{k\neq i}^{K} |\mathbf{h}_i^H \mathbf{w}_k|^2 + \sum_{j=1}^{J} p_j |\ell_{j,i}|^2 + \sigma_i^2}. \tag{7}$$

Thus, based on the DL SINR expression in (7) the MOOP based on IS can be mathematically formulated as

$$\begin{aligned} \mathrm{P}(1): \min_{\{\mathbf{w}_i\},\{p_j\}} \; & c_1 \cdot E_{off} + c_2 \cdot \sum_{j=1}^{J} T_j^{\mathrm{total}} \\ \text{s.t.} \quad & \mathrm{A1}: \frac{q_j}{r_j} + \frac{q_j L_{\mathrm{BS},j}}{f_{\mathrm{BS}}} \leq T_j, \forall j, \\ & \mathrm{A2}: \Gamma_i^{\mathrm{DL}} \geq \Gamma_i, \forall i, \\ & \mathrm{A3}: 0 \leq p_j \leq P_{\max}^{\mathrm{MD}}, \forall j, \\ & \mathrm{A4}: \sum_{i=1}^{K} \|\mathbf{w}_i\|^2 \leq P_{\max}^{\mathrm{DL}}, \end{aligned} \tag{8}$$

where c_1 and c_2 are the weights given to the two objectives, respectively, with $c_1 + c_2 = 1$. Constraints A1 ensures the total offloading latency of each mobile device does not exceed the required threshold T_j. Constraint A2 ensures a certain QoS for the downlink user and constraints A3 and A4 are the maximum power constraints for each mobile device and for downlink transmission, respectively.

At this point, we emphasize the flexibility provided by the MOOP (8) with respect to optimization variables. There is a strong interdependency between the optimization variables, in that, increasing the transmit power of the mobile devices in order to satisfy the latency constraints increases the co-channel interference (CCI) to the downlink users. At the same time, increasing the downlink transmit power to satisfy the downlink SINR constraints due to the increase in CCI, increases the SI power, which hinders the reception of the offloaded computation tasks.

The optimization problem (8) is non-convex and in general difficult to solve partly due to the fractional objective functions. In order to solve (8), in the following we develop a tractable approach to obtain the optimal resource allocation in an iterative manner.

First, given a fixed power p_j for each mobile device, the problem reduces to obtaining the beamforming vectors for the downlink users. Thus, it can be seen that obtaining the beamforming vectors $\mathbf{w}_i$, for $i = 1, \ldots, K$ in (8) aims at minimizing the downlink transmit power in order minimize the SI power to satisfy the constraints. Thus, this can be obtained by solving the following subproblem

$$\begin{aligned} \mathrm{P}(1.1): \min_{\{\mathbf{w}_i\}} \; & \sum_{i=1}^{K} \|\mathbf{w}_i\|^2 \\ \text{s.t.} \quad & \mathrm{A1},\ \mathrm{A2},\ \mathrm{A4}. \end{aligned} \tag{9}$$

The optimization problem (9) is non-convex but can be easily solved through semidefinite relaxation (SDR). The SDR

formulation of (9) is given by

$$\begin{aligned}\widetilde{\mathrm{P}}(1.1): \min_{\{\mathbf{W}_i\succeq 0\}} \ & \sum_{i=1}^{K}\mathrm{Tr}\{\mathbf{W}_i\}\\ \text{s.t.}\quad \widetilde{\mathrm{A1}}: \ & \tau_j-\gamma_j\le 0,\forall j,\\ \widetilde{\mathrm{A2}}: \ & \frac{\mathrm{Tr}(\mathbf{H}_i\mathbf{W}_i)}{\Gamma_i}\ge\sum_{k\neq i}^{K}\mathrm{Tr}(\mathbf{H}_i\mathbf{W}_k)+\sum_{j=1}^{J}p_j|\ell_{j,i}|^2+\sigma_i^2,\forall i,\\ \widetilde{\mathrm{A4}}: \ & \sum_{i=1}^{K}\mathrm{Tr}(\mathbf{W}_i)\le P_{\max}^{\mathrm{DL}},\end{aligned} \tag{10}$$

where $\tau_j=2^{\frac{q_j}{B\left(T_j-\frac{q_jL_{\mathrm{BS},j}}{f_{\mathrm{BS}}}\right)}}-1$.

The SDR formulation (10) is convex and can be solved by standard convex solvers. Please note that, the formulation in (10) is a relaxed form of (9) where the rank one constraint on $\mathbf{W}_i$ has been dropped. If the resulting solution $\mathbf{W}_i$ after solving (10) is rank one, the optimal $\mathbf{w}_i$ can be obtained by applying eigenvalue-decomposition (EVD), otherwise, ramdomization technique [28] can be used to retrieve $\mathbf{w}_i$.

Accordingly, for fixed downlink beamforming vectors $\mathbf{w}_i$, for $i=1,\ldots,K$, the transmit power for the mobile devices can be obtained by solving the following subproblem

$$\begin{aligned}\mathrm{P}(1.2): \min_{\substack{\{p_j\},\{a_j\},\\ \{b_j\}}} \ & c_1\cdot\left(\sum_{j=1}^{J}q_ja_j\right)+c_2\cdot\left(\sum_{j=1}^{J}q_jb_j\right)\\ \text{s.t.}\quad & \mathrm{A5}: \frac{p_j}{r_j}\le a_j,\quad \mathrm{A6}: \frac{1}{r_j}\le b_j,\\ & \widetilde{\mathrm{A1}}: \tau_j-\gamma_j\le 0,\forall j,\\ & \mathrm{A3}: 0\le p_j\le P_{\max}^{\mathrm{MD}},\forall j.\end{aligned} \tag{11}$$

Here, we introduce auxiliary variables a_j and b_j for $j=1,\ldots,J$. In order to solve (11) we analyse the problem using Lagrangian method. Thus, the Lagrange function of problem (11) is

$$\begin{aligned}\mathcal{L}\left(p_j,a_j,b_j,\lambda_j,\mu_j,\beta_j,\nu_j\right)&=c_1\sum_{j=1}^{J}q_ja_j+c_2\sum_{j=1}^{J}q_jb_j\\ &+\sum_{j=1}^{J}\lambda_j\left(p_j-a_jr_j\left(\mathbf{w}_i,p_j\right)\right)+\sum_{j=1}^{J}\mu_j\left(1-b_jr_j\left(\mathbf{w}_i,p_j\right)\right)\\ &+\sum_{j=1}^{J}\beta_j\left(\tau_j-\gamma_j\left(\mathbf{w}_i,p_j\right)\right)+\sum_{j=1}^{J}\nu_j\left(p_j-P_{\max}^{\mathrm{MD}}\right),\end{aligned} \tag{12}$$

where $\lambda_j,\mu_j,\beta_j,\nu_j$ are the Lagrange multipliers for constraints A5, A6, $\widetilde{\mathrm{A1}}$ and A3, respectively. Based on the definition of Karush-Kuhn-Tucker (KKT) conditions, we have

$$\frac{\partial\mathcal{L}}{\partial p_j}=\lambda_j-\lambda_ja_j\frac{\partial r_j}{\partial p_j}-\mu_jb_j\frac{\partial r_j}{\partial p_j}-\beta_j\frac{\partial\gamma_j}{\partial p_j}+\nu_j=0, \tag{13}$$

$$\frac{\partial\mathcal{L}}{\partial a_j}=c_1q_j-\lambda_jr_j=0,\quad \frac{\partial\mathcal{L}}{\partial b_j}=c_2q_j-\mu_jr_j=0, \tag{14}$$

$$\lambda_j\left(p_j-a_jr_j\right)=0,\quad \mu_j\left(1-b_jr_j\right)=0, \tag{15}$$

$$\beta_j\left(\tau_j-\gamma_j\right)=0,\quad \nu_j\left(p_j-P_{\max}^{\mathrm{MD}}\right)=0. \tag{16}$$

From (14) and (15) we have $\lambda_j=\frac{c_1q_j}{r_j}$, $\mu_j=\frac{c_2q_j}{r_j}$, $a_j=\frac{p_j}{r_j}$ and $b_j=\frac{1}{r_j}$, respectively. Furthermore, notice that the optimal solution (p_j^*,a_j^*,b_j^*) of problem (11) satisfies the KKT conditions of the following J subproblems

$$\begin{aligned}\min_{p_j}\quad & \lambda_jp_j-\lambda_ja_jr_j\left(\mathbf{w}_i,p_j\right)-\mu_jb_jr_j\left(\mathbf{w}_i,p_j\right)\\ \text{s.t.}\quad & \widetilde{\mathrm{A1}}: \tau_j-\gamma_j\le 0,\\ & \mathrm{A3}: 0\le p_j\le P_{\max}^{\mathrm{MD}}.\end{aligned} \tag{17}$$

It is easy to see that the KKT conditions for the subproblem (17) are the same as that of problem (11) and are given by

$$\lambda_j-\lambda_ja_j\frac{B}{\ln 2}\frac{\Xi_j}{(1+\gamma_j)}-\mu_jb_j\frac{B}{\ln 2}\frac{\Xi_j}{(1+\gamma_j)}-\beta_j\Xi_j+\nu_j=0, \tag{18}$$

$$\beta_j\left(\tau_j-\gamma_j\right)=0, \tag{19}$$

$$\nu_j\left(p_j-P_{\max}^{\mathrm{MD}}\right)=0. \tag{20}$$

where $\Xi_j=\frac{\left|\mathbf{g}_j^H\mathbf{u}_j\right|^2}{s_j+\sigma_j^2\|\mathbf{u}_j\|^2}$. From (18), we see that the optimal p_j^* is

$$p_j^*=\frac{B}{\ln 2}\frac{\lambda_ja_j+\mu_jb_j}{\lambda_j-\beta_j^*\Xi_j+\nu_j^*}-\frac{1}{\Xi_j}, \tag{21}$$

where β_j^* and ν_j^* satisfy the KKT conditions (19) and (20), respectively. In the following, we examine 3 cases in order to obtain $\{p_j^*,\beta_j^*,\nu_j^*\}$:

1) From (19) and (20) we have $p_j^*\in\left(\frac{\tau_j}{\Xi_j},P_{\max}^{\mathrm{MD}}\right)$ for $\beta_j^*=\nu_j^*=0$. In this case, $p_j^*=M_j$ where $M_j=\frac{B}{\ln 2}\frac{\lambda_ja_j+\mu_jb_j}{\lambda_j}-\frac{1}{\Xi_j}$ according to (21). Thus, we have $p_j^*=M_j$ and $\beta_j^*=\nu_j^*=0$ if $M_j\in\left[\frac{\tau_j}{\Xi_j},P_{\max}^{\mathrm{MD}}\right]$.
2) If $M_j<\frac{\tau_j}{\Xi_j}$ implies that $\beta_j^*>0$ from the constraints (21). Therefore, $p_j^*=\frac{\tau_j}{\Xi_j}$ and $\nu_j^*=0$ according to (19) and (20). By substituting these in (21) gives $\beta_j^*=\frac{\lambda_j}{\Xi_j}-\frac{B}{\ln 2}\frac{\lambda_ja_j+\mu_jb_j}{\tau_j+1}$.
3) Similarly, if $M_j>P_{\max}^{\mathrm{MD}}$ implies that $\nu_j^*>0$. In this case, $p_j^*=P_{\max}^{\mathrm{MD}}$ and $\beta_j^*=0$ according to (20) and (19) and putting these into (21) gives $\nu_j^*=\frac{B}{\ln 2}\frac{\Xi_j(\lambda_ja_j+\mu_jb_j)}{P_{\max}^{\mathrm{MD}}\Xi_j+1}-\lambda_j$.

Accordingly, from these cases the solution to the subproblem shown in (11) is given by

$$p_j^*=\begin{cases}\frac{\tau_j}{\Xi_j}, & \text{for } M_j<\frac{\tau_j}{\Xi_j},\\ M_j, & \text{for } \frac{\tau_j}{\Xi_j}\le M_j\le P_{\max}^{\mathrm{MD}},\\ P_{\max}^{\mathrm{MD}}, & \text{for } M_j>P_{\max}^{\mathrm{MD}},\end{cases} \tag{22}$$

$$\beta_j^*=\begin{cases}\frac{\lambda_j}{\Xi_j}-\frac{B}{\ln 2}\frac{\lambda_ja_j+\mu_jb_j}{\tau_j+1}, & \text{for } M_j<\frac{\tau_j}{\Xi_j},\\ 0, & \text{elsewhere,}\end{cases} \tag{23}$$

$$\nu_j^*=\begin{cases}0, & \text{for } M_j\le P_{\max}^{\mathrm{MD}},\\ \frac{B}{\ln 2}\frac{\Xi_j(\lambda_ja_j+\mu_jb_j)}{P_{\max}^{\mathrm{MD}}\Xi_j+1}-\lambda_j, & \text{elsewhere.}\end{cases} \tag{24}$$

Algorithm 1 summarizes the step by step procedure for solving the optimization (8) based on IS.

Algorithm 1 Iterative algorithm for solving problem (8)

1: **Initialization:**
Set $p_j = P_{\max}^{\mathrm{MD}}$, for $j = 1, \ldots, J$,
Obtain $\mathbf{w}_i$, for $i = 1, \ldots, K$, by solving subproblem (10)
Repeat
Loop
2: Compute λ_j, μ_j, a_j and b_j, for $j = 1, \ldots, J$,
3: Update p_j, β_j and ν_j, for $j = 1, \ldots, J$,
until convergence. End Loop
4: Update $\mathbf{w}_i$, for $i = 1, \ldots, K$ through solving (10)
Until stopping criterion is satisfied.
5: **Output**: $\{\mathbf{w}_i^*\}$ and $\{p_j^*\}$.

B. Trade-off Optimization based on Constructive Interference

In this section, we formulate the MOOP based on constructive interference (CI). The basic idea of CI is that, the knowledge of the downlink data signals at the FD BS can be used to exploit the multiuser interference rather than suppress it as in the conventional case. The concept of CI has been thoroughly studied in the literature for both PSK and QAM modulation in [29]–[38] and references therein, where analytical criteria are also derived. For notational convenience, we focus on PSK here. To formulate the MOOP based on CI, we first write the received symbol at the *i-th* downlink user as

$$\widetilde{y}_i = \mathbf{h}_i^H \left(\sum_{k=1}^{K} \mathbf{w}_k e^{j(\phi_k - \phi_i)} \right) = \mathbf{h}_i^H \mathbf{x}, \tag{25}$$

where we have omitted the noise term, $\mathbf{x} = \sum_{k=1}^{K} \mathbf{w}_k e^{j(\phi_k - \phi_i)}$ and the unit-energy PSK symbol for the *i-th* downlink user is represented as $d_i = de^{\phi_i}$.

As detailed in [32], for any given PSK constellation point, to guarantee CI, $\widetilde{y}_i$ must fall within the CI region of the constellation. The size of the region is determined by $\theta = \pm\frac{\pi}{Y}$, which is the maximum angle shift within the CI region for a modulation order Y. Accordingly, the downlink SINR constraint that guarantees CI at the *i-th* downlink user [32] is

$$|\Im(\widetilde{y}_i)| \leq \left(\Re(\widetilde{y}_i) - \sqrt{\Gamma_i \sum_{j=1}^{J} p_j^{\mathrm{CI}} |\ell_{j,i}|^2 + \Gamma_i \sigma_i^2} \right) \tan\theta, \tag{26}$$

where $\Re$ and $\Im$ are the real and imaginary parts, respectively. Therefore, the MOOP based on CI can be mathematically formulated as

$$\begin{aligned} \mathrm{P}(2): \min_{\mathbf{x}, \{p_j^{\mathrm{CI}}\}} \quad & c_1 \cdot E_{off}^{\mathrm{CI}} + c_2 \cdot \sum_{j=1}^{J} T_j^{\text{total-CI}} \\ \text{s.t.} \quad & \mathrm{B1}: \frac{q_j}{r_j^{\mathrm{CI}}} + \frac{q_j L_{\mathrm{BS},j}}{f_{\mathrm{BS}}} \leq T_j, \forall j, \\ & \mathrm{B2}: (26), \forall i, \\ & \mathrm{B3}: p_j^{\mathrm{CI}} \leq P_{\max}^{\mathrm{MD}}, \forall j, \quad \mathrm{B4}: \|\mathbf{x}\|^2 \leq P_{\max}^{\mathrm{DL}}. \end{aligned} \tag{27}$$

Here, $T_j^{\text{total-CI}} = \frac{q_j}{r_j^{\mathrm{CI}}} + \frac{q_j L_{\mathrm{BS},j}}{f_{\mathrm{BS}}}$ and $E_{off}^{\mathrm{CI}} = \sum_{j=1}^{J} p_j^{\mathrm{CI}} t_{off,j}^{\mathrm{CI}}$, where $r_j^{\mathrm{CI}} = B \log_2\left(1 + \gamma_j^{\mathrm{CI}}\right)$, $\gamma_j^{\mathrm{CI}} = \frac{p_j \left|\mathbf{g}_j^H \mathbf{u}_j\right|^2}{s_j^{\mathrm{CI}} + \sigma_j^2 \|\mathbf{u}_j\|^2}$ and $s_j^{\mathrm{CI}} = \left|\mathbf{u}_j^H \mathbf{H}_{\mathbf{SI}} \mathbf{x}\right|^2$. The MOOP (27) is non-convex. We solve (27) in a similar fashion to Section III-A.

For fixed power p_j^{CI}, the variable $\{\mathbf{x}\}$ can be obtained by solving the following subproblem

$$\begin{aligned} \mathrm{P}(2.1): \min_{\mathbf{x}} \quad & \|\mathbf{x}\|^2 \\ \text{s.t.} \quad & \mathrm{B1}, \mathrm{B2}, \mathrm{B4}. \end{aligned} \tag{28}$$

Unlike the conventional scheme, the subproblem (28) is convex and can be solved using standard convex solvers. Accordingly, given the variable $\{\mathbf{x}\}$, the transmit power for the mobile devices can be obtained by solving the following subproblem

$$\begin{aligned} \mathrm{P}(2.2): \min_{\substack{\{p_j^{\mathrm{CI}}\}, \{a_j^{\mathrm{CI}}\}, \\ \{b_j^{\mathrm{CI}}\}}} \quad & c_1 \cdot \left(\sum_{j=1}^{J} q_j a_j^{\mathrm{CI}} \right) + c_2 \cdot \left(\sum_{j=1}^{J} q_j b_j^{\mathrm{CI}} \right) \\ \text{s.t.} \quad & \mathrm{B5}: \frac{p_j^{\mathrm{CI}}}{r_j^{\mathrm{CI}}} \leq a_j^{\mathrm{CI}}, \quad \mathrm{B6}: \frac{1}{r_j^{\mathrm{CI}}} \leq b_j^{\mathrm{CI}}, \\ & \widetilde{\mathrm{B1}}: \tau_j - \gamma_j^{\mathrm{CI}} \leq 0, \forall j, \\ & \mathrm{B3}: p_j^{\mathrm{CI}} \leq P_{\max}^{\mathrm{MD}}, \forall j, \end{aligned} \tag{29}$$

To solve (29), we analyse the problem using Lagrangian method in a similar fashion to Section III-A. Accordingly, we obtain the following as the corresponding solutions to the problem (29)

$$\lambda_j^{\mathrm{CI}} = \frac{c_1 q_j}{r_j^{\mathrm{CI}}}, \; \mu_j^{\mathrm{CI}} = \frac{c_2 q_j}{r_j^{\mathrm{CI}}}, \; a_j^{\mathrm{CI}} = \frac{p_j^{\mathrm{CI}}}{r_j^{\mathrm{CI}}}, \; b_j^{\mathrm{CI}} = \frac{1}{r_j^{\mathrm{CI}}},$$

$$p_j^{\mathrm{CI}^*} = \begin{cases} \frac{\tau_j}{\Xi_j^{\mathrm{CI}}}, & \text{for } M_j^{\mathrm{CI}} < \frac{\tau_j}{\Xi_j^{\mathrm{CI}}}, \\ M_j^{\mathrm{CI}}, & \text{for } \frac{\tau_j}{\Xi_j^{\mathrm{CI}}} \leq M_j^{\mathrm{CI}} \leq P_{\max}^{\mathrm{MD}}, \\ P_{\max}^{\mathrm{MD}}, & \text{for } M_j^{\mathrm{CI}} > P_{\max}^{\mathrm{MD}}, \end{cases}$$

$$\beta_j^{\mathrm{CI}^*} = \begin{cases} \frac{\lambda_j^{\mathrm{CI}}}{\Xi_j^{\mathrm{CI}}} - \frac{B}{\ln 2} \frac{\lambda_j^{\mathrm{CI}} a_j^{\mathrm{CI}} + \mu_j^{\mathrm{CI}} b_j^{\mathrm{CI}}}{\tau_j + 1}, & \text{for } M_j^{\mathrm{CI}} < \frac{\tau_j}{\Xi_j^{\mathrm{CI}}}, \\ 0, & \text{elsewhere}, \end{cases}$$

$$\nu_j^{\mathrm{CI}^*} = \begin{cases} 0, & \text{for } M_j^{\mathrm{CI}} \leq P_{\max}^{\mathrm{MD}}, \\ \frac{B}{\ln 2} \frac{\Xi_j^{\mathrm{CI}} (\lambda_j^{\mathrm{CI}} a_j^{\mathrm{CI}} + \mu_j^{\mathrm{CI}} b_j^{\mathrm{CI}})}{P_{\max}^{\mathrm{MD}} \Xi_j^{\mathrm{CI}} + 1} - \lambda_j^{\mathrm{CI}}, & \text{elsewhere}, \end{cases}$$

where $\Xi_j^{\mathrm{CI}} = \frac{\left|\mathbf{g}_j^H \mathbf{u}_j\right|^2}{s_j^{\mathrm{CI}} + \sigma_j^2 \|\mathbf{u}_j\|^2}$ and $M_j^{\mathrm{CI}} = \frac{B}{\ln 2} \frac{\lambda_j^{\mathrm{CI}} a_j^{\mathrm{CI}} + \mu_j^{\mathrm{CI}} b_j^{\mathrm{CI}}}{\lambda_j^{\mathrm{CI}}} - \frac{1}{\Xi_j^{\mathrm{CI}}}$. Please note that, a summary of the Algorithm to solve (27) based on CI is omitted, however, (27) can be solved by following the same steps as shown in Algorithm 1 with the corresponding CI based solutions shown in Section III-B.

IV. MOOP Designs based on Imperfect CSI

In the previous section, it is assumed that the FD BS has perfect knowledge of the CSI for all the channel links. However, in practice this is not always the case. Thus, in this section in order to investigate the robustness of the considered system, we extend the MOOP algorithm designs in

the previous section to accommodate for the case where the FD BS does not have perfect CSI knowledge of the channel links.

In the literature, robust designs can generally be categorized into two main designs: the probabilistic and the deterministic based designs. In probabilistic based designs, the error in the CSI knowledge is assumed to have a certain statistical characteristic like the mean or covariance of the channel. In deterministic based designs, which is adopted in this Section, the error in the CSI is assumed to belong to a given uncertainty set. The size of the set determines the amount of uncertainty on the channel and the system optimizes the worst-case performance which achieves a guaranteed performance level for any channel realization in the set. Therefore, for convenience and to avoid any statistical assumptions on the channel, we adopt the worst-case approach which corresponds well to quantization errors and is also suitable for handling slow-fading channels [39].

Accordingly, to model the imperfect CSI, we assume that the actual channels $\mathbf{h}_i, \ell_{j,i}, \mathbf{H}_{\mathrm{SI}}$ and $\mathbf{g}_j$, for $i = 1, \ldots, K$ and $j = 1, \ldots, J$, respectively, lie in the neighbourhood of the estimated channels $\hat{\mathbf{h}}_i, \hat{\ell}_{j,i}, \hat{\mathbf{H}}_{\mathrm{SI}}$ and $\hat{\mathbf{g}}_j$, for $i = 1, \ldots, K$ and $j = 1, \ldots, J$, respectively. Hence, the actual channels are modelled as

$$\begin{aligned}
&\mathbf{h}_i = \hat{\mathbf{h}}_i + \mathbf{e}_{h,i}, \text{ such that } \left\|\mathbf{e}_{h,i}\right\| \leq \epsilon_{h,i}, \forall i,\\
&\ell_{j,i} = \hat{\ell}_{j,i} + e_{j,i}, \text{ such that } \left|e_{j,i}\right| \leq \epsilon_{j,i}, \forall j, i,\\
&\mathbf{g}_j = \hat{\mathbf{g}}_j + \mathbf{e}_{g,j}, \text{ such that } \left\|\mathbf{e}_{g,j}\right\| \leq \epsilon_{g,j}, \forall j,\\
&\mathbf{H}_{\mathrm{SI}} = \hat{\mathbf{H}}_{\mathrm{SI}} + \mathbf{E}_{\mathrm{SI}} \text{ such that } \|\mathbf{E}_{\mathrm{SI}}\|_F \leq \epsilon_{\mathrm{SI}},
\end{aligned}$$

where $\mathbf{e}_{h,i}, e_{j,i}, \mathbf{e}_{g,j}$ and $\mathbf{E}_{\mathrm{SI}}$ represent the channel uncertainties that are assumed to be bounded. We assume the FD BS has no knowledge of the channel uncertainties except their bounds, hence, we take the worst case approach for our algorithm designs. In the following subsections, we present the robust solutions for the proposed interference suppression and interference exploitation designs presented in Section III.

A. Robust Trade-off Design based on IS

The robust formulation of the MOOP based on IS in (8) can be expressed as

$$\begin{aligned}
\mathrm{P}(3): \min_{\{\mathbf{w}_i\},\{p_j\}} \; & c_1 \cdot \hat{E}_{off} + c_2 \cdot \sum_{j=1}^{J} \hat{T}_j^{\mathrm{total}}\\
\text{s.t.} \quad & \mathrm{C1}: \frac{q_j}{\hat{r}_j} + \frac{q_j L_{\mathrm{BS},j}}{f_{\mathrm{BS}}} \leq T_j, \forall \left\|\mathbf{e}_{g,j}\right\| \leq \epsilon_{g,j}, \|\mathbf{E}_{\mathrm{SI}}\|_F \leq \epsilon_{\mathrm{SI}}, \forall j,\\
& \mathrm{C2}: \hat{\Gamma}_i^{\mathrm{DL}} \geq \Gamma_i, \forall \left\|\mathbf{e}_{h,i}\right\| \leq \epsilon_{h,i}, \left\|e_{j,i}\right\| \leq \epsilon_{j,i}, \forall i,\\
& \mathrm{C3}: 0 \leq p_j \leq P_{\max}^{\mathrm{MD}}, \forall j, \quad \mathrm{C4}: \sum_{i=1}^{K} \|\mathbf{w}_i\|^2 \leq P_{\max}^{\mathrm{DL}},
\end{aligned} \tag{30}$$

where we have

$$\hat{\Gamma}_i^{\mathrm{DL}} = \frac{\left|\left(\hat{\mathbf{h}}_i + \mathbf{e}_{h,i}\right)^H \mathbf{w}_i\right|^2}{\sum_{k\neq i}^{K}\left|\left(\hat{\mathbf{h}}_i + \mathbf{e}_{h,i}\right)^H \mathbf{w}_k\right|^2 + \sum_{j=1}^{J} p_j \left|\hat{\ell}_{j,i} + e_{j,i}\right|^2 + \sigma_i^2},$$

$$\hat{\gamma}_j = \frac{p_j \left|\left(\hat{\mathbf{g}}_j + \mathbf{e}_{g,j}\right)^H \mathbf{u}_j\right|^2}{\sum_{n\neq j}^{J} p_n \left|\left(\hat{\mathbf{g}}_n + \mathbf{e}_{g,n}\right)^H \mathbf{u}_j\right|^2 + \hat{s}_j + \sigma_j^2 \left\|\mathbf{u}_j\right\|^2},$$

$$\hat{s}_j = \sum_{i=1}^{K} \left|\mathbf{u}_j^H \left(\hat{\mathbf{H}}_{\mathrm{SI}} + \mathbf{E}_{\mathrm{SI}}\right) \mathbf{w}_i\right|^2,$$

$$\hat{r}_j = B \log_2\left(1 + \hat{\gamma}_j\right),$$

$$\hat{E}_{off} = \sum_{j=1}^{J} p_j \hat{t}_{off,j},$$

$$\sum_{j=1}^{J} \hat{T}_j^{\mathrm{total}} = \frac{q_j}{\hat{r}_j} + \frac{q_j L_{\mathrm{BS},j}}{f_{\mathrm{BS}}}.$$

The formulation in (30) is evidently a non-convex problem, in addition, it contains many inequalities that makes the worst-case design particularly challenging to solve. To solve (30), we simply follow the algorithm design in Section III-A. Hence, the SDR formulations of constraint C1 and C2 can be written respectively as

$$\frac{p_j \left|\left(\hat{\mathbf{g}}_j + \mathbf{e}_{g,j}\right)^H \mathbf{u}_j\right|^2}{\sum_{n\neq j}^{J} p_n \left|\left(\hat{\mathbf{g}}_n + \mathbf{e}_{g,n}\right)^H \mathbf{u}_j\right|^2 + \hat{s}_j^{\mathrm{SI}} + \sigma_j^2 \left\|\mathbf{u}_j\right\|^2} \geq \tau_j, \tag{31}$$

where $\hat{s}_j^{\mathrm{SI}} = \mathrm{Tr}\left\{\left(\hat{\mathbf{H}}_{\mathrm{SI}} + \mathbf{E}_{\mathrm{SI}}\right) \sum_{i=1}^{K} \mathbf{W}_i \left(\hat{\mathbf{H}}_{\mathrm{SI}} + \mathbf{E}_{\mathrm{SI}}\right)^H \mathbf{U}_j\right\}$, and

$$\frac{\left(\hat{\mathbf{h}}_i + \mathbf{e}_{h,i}\right)^H \mathbf{W}_i \left(\hat{\mathbf{h}}_i + \mathbf{e}_{h,i}\right)}{\sum_{k\neq i}^{K}\left(\hat{\mathbf{h}}_i + \mathbf{e}_{h,i}\right)^H \mathbf{W}_k \left(\hat{\mathbf{h}}_i + \mathbf{e}_{h,i}\right) + \sum_{j=1}^{J} p_j \left|\hat{\ell}_{j,i} + e_{j,i}\right|^2 + \sigma_i^2} \geq \Gamma_i. \tag{32}$$

Therefore, the robust formulation of (10) becomes

$$\begin{aligned}
\mathrm{P}(3.1): \min_{\{\mathbf{W}_i \succeq 0\}} \; & \sum_{i=1}^{K} \mathrm{Tr}\left\{\mathbf{W}_i\right\}\\
\text{s.t.} \quad & \overline{\mathrm{C1}}: (31), \forall \left\|\mathbf{e}_{g,j}\right\| \leq \epsilon_{g,j}, \|\mathbf{E}_{\mathrm{SI}}\|_F \leq \epsilon_{\mathrm{SI}}, \forall j,\\
& \overline{\mathrm{C2}}: (32), \forall \left\|\mathbf{e}_{h,i}\right\| \leq \epsilon_{h,i}, \left\|e_{j,i}\right\| \leq \epsilon_{j,i}, \forall i,\\
& \overline{\mathrm{C4}}: \sum_{i=1}^{K} \mathrm{Tr}\left(\mathbf{W}_i\right) \leq P_{\max}^{\mathrm{DL}}.
\end{aligned} \tag{33}$$

To make (33) more tractable to analyze and solve, we first simplify and relax part of constraints $\overline{\mathrm{C1}}$ and $\overline{\mathrm{C2}}$, and then transform them into linear matrix inequalities (LMIs) using the so-called S-procedure [40]. First, notice that $\overline{\mathrm{C1}}$ can be simplified by introducing auxiliary variables such that $\overline{\mathrm{C1}}$ can be written as the following two constraints

$$p_j \left|\left(\hat{\mathbf{g}}_j + \mathbf{e}_{g,j}\right)^H \mathbf{u}_j\right|^2 \geq \tau_j \left(\sum_{n\neq j}^{J} p_n \left|\left(\hat{\mathbf{g}}_n + \mathbf{e}_{g,n}\right)^H \mathbf{u}_j\right|^2 + \hat{S}_j^{\mathrm{SI}}\right), \tag{34}$$

$$\mathrm{Tr}\left\{\left(\hat{\mathbf{H}}_{\mathrm{SI}} + \mathbf{E}_{\mathrm{SI}}\right) \sum_{i=1}^{K} \mathbf{W}_i \left(\hat{\mathbf{H}}_{\mathrm{SI}} + \mathbf{E}_{\mathrm{SI}}\right)^H \mathbf{U}_j\right\} + \sigma_j^2 \left\|\mathbf{u}_j\right\|^2 \leq \hat{S}_j^{\mathrm{SI}}. \tag{35}$$

By using the inequalities $\left|\mathbf{x}^H\mathbf{y}\right| \leq \|\mathbf{x}\|\,\|\mathbf{y}\|$ and $\|\mathbf{x}+\mathbf{y}\|^2 \leq (\|\mathbf{x}\|+\|\mathbf{y}\|)^2$, (34) can be relaxed to the following robust formulation

$$p_j\left(|\hat{\mathbf{g}}_j^H\mathbf{u}_j| + \epsilon_{g,j}\|\mathbf{u}_j\|\right)^2 \geq \tau_j\left(\sum_{n\neq j}^{J} p_n\left(|\hat{\mathbf{g}}_n^H\mathbf{u}_j| + \epsilon_{g,n}\|\mathbf{u}_j\|\right)^2 + \hat{S}_j^{\mathrm{SI}}\right), \forall j. \tag{36}$$

Also, notice that $\overline{\mathrm{C2}}$ can be simplified to the following two constraints,

$$\left(\hat{\mathbf{h}}_i + \mathbf{e}_{h,i}\right)^H \mathbf{Q}_i\left(\hat{\mathbf{h}}_i + \mathbf{e}_{h,i}\right) - \Gamma_i\left(L_i + \sigma_i^2\right) \geq 0, \tag{37}$$

$$\sum_{j=1}^{J} p_j\left|\hat{\ell}_{j,i} + e_{j,i}\right|^2 \leq L_i, \tag{38}$$

where $\mathbf{Q}_i = \mathbf{W}_i - \Gamma_i\sum_{k\neq i}^{K}\mathbf{W}_k$. (38) can be relaxed to give the following robust formultion

$$\sum_{j=1}^{J} p_j\left(\left|\hat{\ell}_{j,i}\right| + \epsilon_{j,i}\right)^2 \leq L_i, \forall i. \tag{39}$$

Next, we transform the constraints (35) and (37) to LMIs. Towards this end, we review the definition of the S-procedure [40] for completeness.

Lemma 1. (S-procedure [40]): Let $g_l(\mathbf{x})$, $l = 1, 2$, be defined as

$$g_l(\mathbf{x}) = \mathbf{x}^H\mathbf{A}_l\mathbf{x} + 2Re\left\{\mathbf{b}_l^H\mathbf{x}\right\} + c_l,$$

where $\mathbf{A}_l \in \mathbb{C}^{n\times n}, \mathbf{b}_l \in \mathbb{C}^n$ and $c_l \in \mathbb{R}$. Then, the implication of $g_1(\mathbf{x}) \geq 0 \Rightarrow g_2(\mathbf{x}) \geq 0$ holds if and only if there exists a $\lambda \geq 0$ such that

$$\lambda\begin{bmatrix}\mathbf{A}_1 & \mathbf{b}_1\\ \mathbf{b}_1^H & c_1\end{bmatrix} - \begin{bmatrix}\mathbf{A}_2 & \mathbf{b}_2\\ \mathbf{b}_2^H & c_2\end{bmatrix} \geq 0,$$

provided there exists a point $\hat{\mathbf{x}}$ with $g_1(\hat{\mathbf{x}}) > 0$.

To apply the S-procedure, we expand constraints (35) and (37) by using the fact that $\mathrm{Tr}\{\mathbf{ABCD}\} = \mathrm{vec}\left(\mathbf{A}^H\right)^H\left(\mathbf{D}^H\otimes\mathbf{B}\right)\mathrm{vec}\left(\mathbf{C}\right)$ as follows

$$\mathbf{e}_{\mathrm{SI}}^H\left(\mathbf{U}_j\otimes\sum_{k=1}^{K}\mathbf{W}_k\right)\mathbf{e}_{\mathrm{SI}} + 2Re\left\{\hat{\mathbf{h}}_{\mathrm{SI}}^H\left(\mathbf{U}_j\otimes\sum_{k=1}^{K}\mathbf{W}_k\right)\mathbf{e}_{\mathrm{SI}}\right\} + \hat{\mathbf{h}}_{\mathrm{SI}}^H\left(\mathbf{U}_j\otimes\sum_{k=1}^{K}\mathbf{W}_k\right)\hat{\mathbf{h}}_{\mathrm{SI}}^H + \sigma_j^2\mathrm{Tr}\left\{\mathbf{U}_j\right\} - \hat{S}_j^{\mathrm{SI}} \leq 0 \tag{40}$$

$$\mathbf{e}_{h,i}^H\mathbf{Q}_i\mathbf{e}_{h,i} + 2Re\left\{\hat{\mathbf{h}}_i^H\mathbf{Q}_i\mathbf{e}_{h,i}\right\} + \hat{\mathbf{h}}_i^H\mathbf{Q}_i\hat{\mathbf{h}}_i - \Gamma_i\left(L_i + \sigma_i^2\right) \geq 0, \tag{41}$$

We denote $\hat{\mathbf{h}}_{\mathrm{SI}} = \mathrm{vec}\left(\hat{\mathbf{H}}_{\mathrm{SI}}^H\right)$ and $\mathbf{e}_{\mathrm{SI}} = \mathrm{vec}\left(\mathbf{E}_{\mathrm{SI}}^H\right)$ where, $\mathrm{vec}\left(\cdot\right)$ stacks the columns of a matrix into a vector and $\otimes$ stands for Kronecker product. Thus, following Lemma 1, (40) and (41) can be transform into the following LMIs, respectively

$$\begin{bmatrix}\rho\mathbf{I} - Z_j & -Z_j\hat{\mathbf{h}}_{\mathrm{SI}}\\ -\hat{\mathbf{h}}_{\mathrm{SI}}^H Z_j & \hat{S}_j^{\mathrm{SI}} - \hat{\mathbf{h}}_{\mathrm{SI}}^H Z_j\hat{\mathbf{h}}_{\mathrm{SI}} - \sigma_N^2\mathrm{Tr}\left\{\mathbf{U}_j\right\} - \rho\epsilon_{\mathrm{SI}}^2\end{bmatrix} \geq 0, \forall j, \tag{42}$$

where $Z_j = \left(\mathbf{U}_j\otimes\sum_{i=1}^{K}\mathbf{W}_i\right)$, and

$$\begin{bmatrix}\delta_i\mathbf{I} + \mathbf{Q}_i & \mathbf{Q}_i\hat{\mathbf{h}}_i\\ \hat{\mathbf{h}}_i^H\mathbf{Q}_i & \hat{\mathbf{h}}_i^H\mathbf{Q}_i\hat{\mathbf{h}}_i - \Gamma_i\left(L_i + \sigma_i^2\right) - \delta_i\epsilon_{h,i}^2\end{bmatrix} \geq 0, \forall i. \tag{43}$$

Therefore, (33) can be re-expressed as

$$\begin{aligned}\widetilde{\mathrm{P}}(3.1): \min_{\{\mathbf{W}_i\geq 0\}} & \sum_{i=1}^{K}\mathrm{Tr}\left\{\mathbf{W}_i\right\}\\ \text{s.t.} \quad & (36),\quad (39),\quad (42),\quad (43),\quad \overline{\mathrm{C4}}.\end{aligned} \tag{44}$$

The problem (44) is convex and can be solved by standard convex solvers. We note that the formulation in (44) is a relaxed form of (30). If the resulting solution $\mathbf{W}_i$ after solving (44) is rank one, the optimal $\mathbf{w}_i$ can be obtained by applying eigenvalue-decomposition (EVD), otherwise, ramdomization technique [28] can be used to retrieve $\mathbf{w}_i$.

Next, for fixed beamforming vectors the transmit power for the mobile devices can be obtained by solving the following robust subproblem

$$\begin{aligned}\mathrm{P}(3.2): \min_{\substack{\{p_j\},\{\hat{a}_j\},\\ \{\hat{b}_j\}}} & c_1\cdot\left(\sum_{j=1}^{J} q_j\hat{a}_j\right) + c_2\cdot\left(\sum_{j=1}^{J} q_j\hat{b}_j\right)\\ \text{s.t.} \quad & \mathrm{C5}: \frac{p_j}{\hat{r}_j} \leq \hat{a}_j, \quad \mathrm{C6}: \frac{1}{\hat{r}_j} \leq \hat{b}_j,\\ & \widetilde{\mathrm{C1}}: \tau_j - \hat{\gamma}_j \leq 0, \forall j,\\ & \mathrm{C3}: 0 \leq p_j \leq P_{\max}^{\mathrm{MD}}, \forall j.\end{aligned} \tag{45}$$

The Lagrange function of problem (45) is

$$\begin{aligned}\mathcal{L}\left(p_j,\hat{a}_j,\hat{b}_j,\hat{\lambda}_j,\hat{\mu}_j,\hat{\beta}_j,\hat{\nu}_j\right) &= c_1\sum_{j=1}^{J} q_j\hat{a}_j + c_2\sum_{j=1}^{J} q_j\hat{b}_j\\ &+ \sum_{j=1}^{J}\hat{\lambda}_j\left(p_j - \hat{a}_j\hat{r}_j\right) + \sum_{j=1}^{J}\hat{\mu}_j\left(1 - \hat{b}_j\hat{r}_j\right) + \sum_{j=1}^{J}\hat{\beta}_j\left(\tau_j - \hat{\gamma}_j\right)\\ &+ \sum_{j=1}^{J}\hat{\nu}_j\left(p_j - P_{\max}^{\mathrm{MD}}\right),\end{aligned} \tag{46}$$

where $\hat{\lambda}_j, \hat{\mu}_j, \hat{\beta}_j, \hat{\nu}_j$ are Lagrange multipliers. The KKT conditions are given by

$$\begin{aligned}\frac{\partial\mathcal{L}}{\partial p_j} &= \hat{\lambda}_j - \hat{\lambda}_j\hat{a}_j\frac{\partial\hat{r}_j}{\partial p_j} - \hat{\mu}_j\hat{b}_j\frac{\partial\hat{r}_j}{\partial p_j} - \hat{\beta}_j\frac{\partial\hat{\gamma}_j}{\partial p_j} - \sum_{n\neq j}^{J}\hat{\lambda}_n\hat{a}_n\frac{\partial\hat{r}_n}{\partial p_j}\\ &- \sum_{n\neq j}^{J}\hat{\mu}_n\hat{b}_n\frac{\partial\hat{r}_n}{\partial p_j} - \sum_{n\neq j}^{J}\hat{\beta}_n\frac{\partial\hat{\gamma}_n}{\partial p_j} + \hat{\nu}_j = 0,\end{aligned} \tag{47}$$

$$\frac{\partial\mathcal{L}}{\partial\hat{a}_j} = c_1q_j - \hat{\lambda}_j\hat{r}_j = 0, \ \frac{\partial\mathcal{L}}{\partial\hat{b}_j} = c_2q_j - \hat{\mu}_j\hat{r}_j = 0, \tag{48}$$

$$\hat{\lambda}_j\left(p_j - \hat{a}_j\hat{r}_j\right) = 0, \ \hat{\mu}_j\left(1 - \hat{b}_j\hat{r}_j\right) = 0, \tag{49}$$

$$\hat{\beta}_j\left(\tau_j - \hat{\gamma}_j\right) = 0, \ \hat{\nu}_j\left(p_j - P_{\max}^{\mathrm{MD}}\right) = 0. \tag{50}$$

From (48) and (49) we have $\hat{\lambda}_j = \frac{c_1 q_j}{\hat{r}_j}$, $\hat{\mu}_j = \frac{c_2 q_j}{\hat{r}_j}$, $\hat{a}_j = \frac{p_j}{\hat{r}_j}$ and $\hat{b}_j = \frac{1}{\hat{r}_j}$, respectively. Also, we have

$$\frac{\partial \hat{\gamma}_j}{\partial p_j} = \frac{\left|\left(\hat{\mathbf{g}}_j + \mathbf{e}_{g,j}\right)^H \mathbf{u}_j\right|^2}{\sum_{n\neq j}^{J} p_n \left|\left(\hat{\mathbf{g}}_n + \mathbf{e}_{g,n}\right)^H \mathbf{u}_j\right|^2 + \hat{s}_j + \sigma_j^2 \left\|\mathbf{u}_j\right\|^2},$$

$$\frac{\partial \hat{r}_j}{\partial p_j} = \frac{B}{\ln 2\left(1+\hat{\gamma}_j\right)} \cdot \frac{\partial \hat{\gamma}_j}{\partial p_j},$$

$$\frac{\partial \hat{\gamma}_n}{\partial p_j} = -\frac{\hat{\gamma}_n^2 \left|\left(\hat{\mathbf{g}}_j + \mathbf{e}_{g,j}\right)^H \mathbf{u}_n\right|^2}{p_n \left|\left(\hat{\mathbf{g}}_n + \mathbf{e}_{g,n}\right)^H \mathbf{u}_n\right|^2},$$

$$\frac{\partial \hat{r}_n}{\partial p_j} = -\frac{B}{\ln 2\left(1+\hat{\gamma}_n\right)} \cdot \frac{\partial \hat{\gamma}_n}{\partial p_j},$$

which can be relaxed to give the following robust formulations, respectively,

$$\frac{\partial \overline{\gamma}_j}{\partial p_j} = \hat{\Xi}_j, \quad \frac{\partial \overline{r}_j}{\partial p_j} = \frac{B}{\ln 2\left(1+p_j\hat{\Xi}_j\right)} \cdot \hat{\Xi}_j,$$

$$\frac{\partial \overline{\gamma}_n}{\partial p_j} = -\frac{\left(p_n\hat{\Xi}_n\right)^2 \left(|\hat{\mathbf{g}}_j^H \mathbf{u}_n| + \epsilon_{g,j}\|\mathbf{u}_n\|\right)^2}{p_n\left(|\hat{\mathbf{g}}_n^H \mathbf{u}_n| + \epsilon_{g,n}\|\mathbf{u}_n\|\right)^2},$$

$$\frac{\partial \overline{r}_n}{\partial p_j} = -\frac{B}{\ln 2\left(1+p_n\hat{\Xi}_n\right)} \cdot \frac{-\partial \overline{\gamma}_n}{\partial p_j},$$

where $\hat{\Xi}_j = \frac{\left(|\hat{\mathbf{g}}_j^H \mathbf{u}_j| + \epsilon_{g,j}\|\mathbf{u}_j\|\right)^2}{\sum_{n\neq j}^{J} p_n\left(|\hat{\mathbf{g}}_n^H \mathbf{u}_j| + \epsilon_{g,n}\|\mathbf{u}_j\|\right)^2 + \overline{s}_j + \sigma_j^2\|\mathbf{u}_j\|^2}$ and $\overline{s}_j = \sum_{i=1}^{K}\left(|\mathbf{u}_j^H \hat{\mathbf{H}}_{\mathrm{SI}} \mathbf{w}_i| + \epsilon_{\mathrm{SI}}\|\mathbf{u}_j\|\|\mathbf{w}_i\|\right)^2$. Here, we used the inequalities $\left|\mathbf{x}^H\mathbf{y}\right| \leq \|\mathbf{x}\|\,\|\mathbf{y}\|$ and $\|\mathbf{x}+\mathbf{y}\|^2 \leq (\|\mathbf{x}\| + \|\mathbf{y}\|)^2$. Further notice that, the optimal solutions of (45) can be obtained by solving the following J subproblems since they have the same KKT conditions

$$\begin{aligned} \min_{p_j} \quad & \hat{\lambda}_j p_j + D_j p_j - \hat{\lambda}_j \hat{a}_j \hat{r}_j - \hat{\mu}_j \hat{b}_j \hat{r}_j \\ \text{s.t.} \quad & \widetilde{\text{C1}} : \tau_j - \hat{\gamma}_j \leq 0, \\ & \text{C3} : 0 \leq p_j \leq P_{\max}^{\mathrm{MD}}, \end{aligned} \tag{51}$$

where

$$D_j = -\sum_{n\neq j}^{J} \hat{\beta}_n \frac{\partial \overline{\gamma}_n}{\partial p_j} - \sum_{n\neq j}^{J} \hat{\lambda}_n \hat{a}_n \frac{\partial \overline{r}_n}{\partial p_j} - \sum_{n\neq j}^{J} \hat{\mu}_n \hat{b}_n \frac{\partial \overline{r}_n}{\partial p_j}.$$

The KKT conditions are given by

$$\hat{\lambda}_j + D_j - \hat{\lambda}_j \hat{a}_j \frac{\partial \overline{r}_j}{\partial p_j} - \hat{\mu}_j \hat{b}_j \frac{\partial \overline{r}_j}{\partial p_j} - \hat{\beta}_j \frac{\partial \overline{\gamma}_j}{\partial p_j} + \hat{\nu}_j = 0, \tag{52}$$

$$\hat{\beta}_j\left(\tau_j - \hat{\gamma}_j\right) = 0, \tag{53}$$

$$\hat{\nu}_j\left(p_j - P_{\max}^{\mathrm{MD}}\right) = 0. \tag{54}$$

From (52), we have

$$p_j^* = \frac{B}{\ln 2} \frac{\hat{\lambda}_j \hat{a}_j + \hat{\mu}_j \hat{b}_j}{\hat{\lambda}_j + D_j - \hat{\beta}_j^* \hat{\Xi}_j + \hat{\nu}_j^*} - \frac{1}{\hat{\Xi}_j}, \tag{55}$$

where $\hat{\beta}_j^*$ and $\hat{\nu}_j^*$ satisfy the KKT conditions (53) and (54), respectively. After examining the KKT conditions in similar fashion as in Section III-A, we obtain the following optimal solutions

$$p_j^* = \begin{cases} \frac{\tau_j}{\hat{\Xi}_j}, & \text{for } \hat{M}_j < \frac{\tau_j}{\hat{\Xi}_j}, \\ \hat{M}_j, & \text{for } \frac{\tau_j}{\hat{\Xi}_j} \leq \hat{M}_j \leq P_{\max}^{\mathrm{MD}}, \\ P_{\max}^{\mathrm{MD}}, & \text{for } \hat{M}_j > P_{\max}^{\mathrm{MD}}, \end{cases} \tag{56}$$

$$\hat{\beta}_j^* = \begin{cases} \frac{\hat{\lambda}_j + D_j}{\hat{\Xi}_j} - \frac{B}{\ln 2}\frac{\hat{\lambda}_j \hat{a}_j + \hat{\mu}_j \hat{b}_j}{\tau_j + 1}, & \text{for } \hat{M}_j < \frac{\tau_j}{\hat{\Xi}_j}, \\ 0, & \text{elsewhere}, \end{cases} \tag{57}$$

$$\hat{\nu}_j^* = \begin{cases} 0, & \text{for } \hat{M}_j \leq P_{\max}^{\mathrm{MD}}, \\ \frac{B}{\ln 2}\frac{\hat{\Xi}_j(\hat{\lambda}_j \hat{a}_j + \hat{\mu}_j \hat{b}_j)}{P_{\max}^{\mathrm{MD}}\hat{\Xi}_j + 1} - \hat{\lambda}_j - D_j, & \text{elsewhere}, \end{cases} \tag{58}$$

where $\hat{M}_j = \frac{B}{\ln 2}\frac{\hat{\lambda}_j \hat{a}_j + \hat{\mu}_j \hat{b}_j}{\hat{\lambda}_j + D_j} - \frac{1}{\hat{\Xi}_j}$. We note that, the same procedure as shown in Algorithm 1 can be used to solve the robust optimization problem (30) based on IS with the corresponding solutions shown in Section IV-A.

B. Robust Trade-off Design based on CI

For the robust design based on CI, we start by writing the robust formulation of (26) as

$$|\Im\left(\hat{y}_i\right)| \leq \left(\Re(\hat{y}_i) - \sqrt{\Gamma_i \sum_{j=1}^{J} p_j^{\mathrm{CI}} \left|\hat{\ell}_{j,i} + e_{j,i}\right|^2 + \Gamma_i \sigma_i^2}\right) \tan\theta, \tag{59}$$

where $\hat{y}_i = \left(\hat{\mathbf{h}}_i + \mathbf{e}_{h,i}\right)^H \mathbf{x}$. Thus, the robust formulation of (27) becomes

$$\begin{aligned} \mathrm{P}(4): \min_{\mathbf{x}, \{p_j^{\mathrm{CI}}\}} \quad & c_1 \cdot \hat{E}_{off}^{\mathrm{CI}} + c_2 \cdot \sum_{j=1}^{J} \hat{T}_j^{\text{total-CI}} \\ \text{s.t.} \quad & \mathrm{D1} : \frac{q_j}{\hat{r}_j^{\mathrm{CI}}} + \frac{q_j L_{\mathrm{BS},j}}{f_{\mathrm{BS}}} \leq T_j, \forall j, \\ & \mathrm{D2} : (59), \forall i, \\ & \mathrm{D3} : p_j^{\mathrm{CI}} \leq P_{\max}^{\mathrm{MD}}, \forall j, \\ & \mathrm{D4} : \|\mathbf{x}\|^2 \leq P_{\max}^{\mathrm{DL}}. \end{aligned} \tag{60}$$

Here, $\hat{T}_j^{\text{total-CI}} = \frac{q_j}{\hat{r}_j^{\mathrm{CI}}} + \frac{q_j L_{\mathrm{BS},j}}{f_{\mathrm{BS}}}$ and $\hat{E}_{off}^{\mathrm{CI}} = \sum_{j=1}^{J} p_j^{\mathrm{CI}} \hat{t}_{off,j}^{\mathrm{CI}}$, where $\hat{r}_j^{\mathrm{CI}} = B\log_2\left(1+\hat{\gamma}_j^{\mathrm{CI}}\right)$, $\hat{\gamma}_j^{\mathrm{CI}} = \frac{p_j^{\mathrm{CI}}\left|\left(\hat{\mathbf{g}}_j + \mathbf{e}_{g,j}\right)^H \mathbf{u}_j\right|^2}{\sum_{n\neq j}^{J} p_n^{\mathrm{CI}}\left|\left(\hat{\mathbf{g}}_n + \mathbf{e}_{g,n}\right)^H \mathbf{u}_j\right|^2 + \hat{s}_j^{\mathrm{CI}} + \sigma_j^2\|\mathbf{u}_j\|^2}$ and $\hat{s}_j^{\mathrm{CI}} = \left|\mathbf{u}_j^H\left(\hat{\mathbf{H}}_{\mathrm{SI}} + \mathbf{E}_{\mathrm{SI}}\right)\mathbf{x}\right|^2$. Following the algorithm design in Section III-B, for fixed $\{p_j^{\mathrm{CI}}\}$ we obtain $\mathbf{x}$ by solving

$$\begin{aligned} \mathrm{P}(4.1): \min_{\mathbf{x}} \quad & \|\mathbf{x}\|^2 \\ \text{s.t.} \quad & \mathrm{D1}, \mathrm{D2}, \mathrm{D4}. \end{aligned} \tag{61}$$

Problem (61) is non-convex. We solve (61) as follows. First, consider constraint D1 which can be written as

$$p_j^{\mathrm{CI}} \left| \left(\hat{\mathbf{g}}_j + \mathbf{e}_{g,j}\right)^H \mathbf{u}_j \right|^2 \geq \tau_j \left[\sum_{n \neq j}^{J} p_n^{\mathrm{CI}} \left| \left(\hat{\mathbf{g}}_n + \mathbf{e}_{g,n}\right)^H \mathbf{u}_j \right|^2 + \hat{s}_j^{\mathrm{CI}} + \sigma_j^2 \left\|\mathbf{u}_j\right\|^2 \right], \quad (62)$$

which can be relaxed to give the following robust formulation

$$p_j \left(|\hat{\mathbf{g}}_j^H \mathbf{u}_j| + \epsilon_{g,j} \|\mathbf{u}_j\| \right)^2 \geq \tau_j \left[\sum_{n \neq j}^{J} p_n \left(|\hat{\mathbf{g}}_n^H \mathbf{u}_j| + \epsilon_{g,n} \|\mathbf{u}_j\| \right)^2 + \left(|\mathbf{u}_j^H \hat{\mathbf{H}}_{\mathrm{SI}} \mathbf{x}|^2 + \epsilon_{\mathrm{SI}} \|\mathbf{u}_j\| \|\mathbf{x}\| \right)^2 + \sigma_j^2 \left\|\mathbf{u}_j\right\|^2 \right], \forall j. \quad (63)$$

Constraint D2 can be written as

$$\left| (\underline{\hat{\mathbf{h}}}_i + \underline{\mathbf{e}}_{h,i})^H \underline{\mathbf{x}} \right| - \left[(\underline{\hat{\mathbf{h}}}_i + \underline{\mathbf{e}}_{h,i})^H \mathbf{\Pi} \underline{\mathbf{x}} - \sqrt{\Gamma_i \left(\sum_{j=1}^{J} p_j \left| \hat{\ell}_{j,i} + e_{j,i} \right|^2 + \sigma_i^2 \right)} \right] \tan\theta \leq 0, \forall i, \quad (64)$$

which can be relaxed to the following two robust formulations

$$\hat{\underline{\mathbf{h}}}_i^H (\underline{\mathbf{x}} - \mathbf{\Pi} \underline{\mathbf{x}} \tan\theta) + \epsilon_{h,i} \|\underline{\mathbf{x}} - \mathbf{\Pi} \underline{\mathbf{x}} \tan\theta\| + \sqrt{\Gamma_i \left(\sum_{j=1}^{J} p_j \left(\left| \hat{\ell}_{j,i} \right| + \epsilon_{j,i} \right)^2 \right)} \tan\theta \leq 0, \forall i, \quad (65)$$

$$\hat{\underline{\mathbf{h}}}_i^H (-\underline{\mathbf{x}} - \mathbf{\Pi} \underline{\mathbf{x}} \tan\theta) + \epsilon_{h,i} \| - \underline{\mathbf{x}} - \mathbf{\Pi} \underline{\mathbf{x}} \tan\theta\| + \sqrt{\Gamma_i \left(\sum_{j=1}^{J} p_j \left(\left| \hat{\ell}_{j,i} \right| + \epsilon_{j,i} \right)^2 \right)} \tan\theta \leq 0, \forall i, \quad (66)$$

where $\underline{\mathbf{x}} = \left[\Re(\mathbf{x})^H \quad \Im(\mathbf{x}^H)\right]^H$, $\mathbf{\Pi} = \begin{bmatrix} \mathbf{0}_N & -\mathbf{I}_N \\ \mathbf{I}_N & \mathbf{0}_N \end{bmatrix}$, $\hat{\underline{\mathbf{h}}}_i = \left[\Im(\hat{\mathbf{h}}_i)^H \quad \Re(\hat{\mathbf{h}}_i)^H\right]^H$, $\underline{\mathbf{e}}_{h,i} = \left[\Im(\mathbf{e}_{h,i})^H \quad \Re(\mathbf{e}_{h,i})^H\right]^H$. Therefore, problem the transformed problem (61) can be expressed as

$$\widetilde{\mathrm{P}}(4.1): \min_{\mathbf{x}} \quad \|\mathbf{x}\|^2 \quad \text{s.t.} \quad (63), (65), (66), \mathrm{D4}. \quad (67)$$

(67) is convex and can be solved using standard convex solvers.

Accordingly, given the variable $\{\mathbf{x}\}$, the transmit power for the mobile devices can be obtained by solving the following subproblem

$$\mathrm{P}(4.2): \min_{\substack{\{p_j^{\mathrm{CI}}\},\{\hat{a}_j^{\mathrm{CI}}\},\\ \{\hat{b}_j^{\mathrm{CI}}\}}} c_1 \cdot \left(\sum_{j=1}^{J} q_j \hat{a}_j^{\mathrm{CI}} \right) + c_2 \cdot \left(\sum_{j=1}^{J} q_j \hat{b}_j^{\mathrm{CI}} \right) \quad \text{s.t.} \quad \mathrm{D5}: \frac{p_j^{\mathrm{CI}}}{\hat{r}_j^{\mathrm{CI}}} \leq \hat{a}_j^{\mathrm{CI}}, \quad \mathrm{D6}: \frac{1}{\hat{r}_j^{\mathrm{CI}}} \leq \hat{b}_j^{\mathrm{CI}}, \quad (68)$$
$$\widetilde{\mathrm{D1}}: \tau_j - \hat{\gamma}_j^{\mathrm{CI}} \leq 0, \forall j,$$
$$\mathrm{D3}: p_j^{\mathrm{CI}} \leq P_{\max}^{\mathrm{MD}}, \forall j,$$

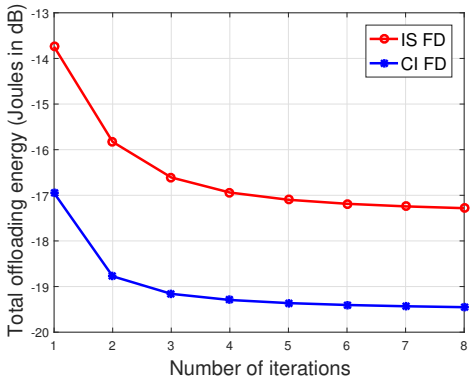

Fig. 2. Total offloading energy vers[width=8cm]us number of iterations.

To solve (68), we analyse the problem using Lagrangian method in a similar fashion to Section IV-A. Accordingly, we obtain the following as the corresponding solutions to the problem (68)

$$\hat{\lambda}_j^{\mathrm{CI}} = \frac{c_1 q_j}{\hat{r}_j^{\mathrm{CI}}}, \ \hat{\mu}_j^{\mathrm{CI}} = \frac{c_2 q_j}{\hat{r}_j^{\mathrm{CI}}}, \ \hat{a}_j^{\mathrm{CI}} = \frac{p_j^{\mathrm{CI}}}{\hat{r}_j^{\mathrm{CI}}}, \ \hat{b}_j^{\mathrm{CI}} = \frac{1}{\hat{r}_j^{\mathrm{CI}}},$$

$$p_j^{\mathrm{CI}^*} = \begin{cases} \frac{\tau_j}{\hat{\Xi}_j^{\mathrm{CI}}}, & \text{for } \hat{M}_j^{\mathrm{CI}} < \frac{\tau_j}{\hat{\Xi}_j^{\mathrm{CI}}}, \\ \hat{M}_j^{\mathrm{CI}}, & \text{for } \frac{\tau_j}{\hat{\Xi}_j^{\mathrm{CI}}} \leq \hat{M}_j^{\mathrm{CI}} \leq P_{\max}^{\mathrm{MD}}, \\ P_{\max}^{\mathrm{MD}}, & \text{for } \hat{M}_j^{\mathrm{CI}} > P_{\max}^{\mathrm{MD}}, \end{cases}$$

$$\hat{\beta}_j^{\mathrm{CI}^*} = \begin{cases} \frac{\hat{\lambda}_j^{\mathrm{CI}} + D_j^{\mathrm{CI}}}{\hat{\Xi}_j^{\mathrm{CI}}} - \frac{B}{\ln 2} \frac{\hat{\lambda}_j^{\mathrm{CI}} \hat{a}_j^{\mathrm{CI}} + \hat{\mu}_j^{\mathrm{CI}} \hat{b}_j^{\mathrm{CI}}}{\tau_j + 1}, & \text{for } \hat{M}_j^{\mathrm{CI}} < \frac{\tau_j}{\hat{\Xi}_j^{\mathrm{CI}}}, \\ 0, & \text{elsewhere,} \end{cases}$$

$$\hat{\nu}_j^{\mathrm{CI}^*} = \begin{cases} 0, & \text{for } \hat{M}_j^{\mathrm{CI}} \leq P_{\max}^{\mathrm{MD}}, \\ \frac{B}{\ln 2} \frac{\hat{\Xi}_j^{\mathrm{CI}} (\hat{\lambda}_j^{\mathrm{CI}} \hat{a}_j^{\mathrm{CI}} + \hat{\mu}_j^{\mathrm{CI}} \hat{b}_j^{\mathrm{CI}})}{P_{\max}^{\mathrm{MD}} \hat{\Xi}_j^{\mathrm{CI}} + 1} - \hat{\lambda}_j^{\mathrm{CI}} - D_j^{\mathrm{CI}}, & \text{elsewhere,} \end{cases}$$

where

$$\hat{\Xi}_j^{\mathrm{CI}} = \frac{\left(|\hat{\mathbf{g}}_j^H \mathbf{u}_j| + \epsilon_{g,j} \|\mathbf{u}_j\| \right)^2}{\sum_{n \neq j}^{J} p_n \left(|\hat{\mathbf{g}}_n^H \mathbf{u}_j| + \epsilon_{g,n} \|\mathbf{u}_j\| \right)^2 + \bar{s}_j^{\mathrm{CI}} + \sigma_j^2 \left\|\mathbf{u}_j\right\|^2},$$

$$\bar{s}_j^{\mathrm{CI}} = \left(|\mathbf{u}_j^H \hat{\mathbf{H}}_{\mathrm{SI}} \mathbf{x}|^2 + \epsilon_{\mathrm{SI}} \|\mathbf{u}_j\| \|\mathbf{x}\| \right)^2,$$

$$\hat{M}_j^{\mathrm{CI}} = \frac{B}{\ln 2} \frac{\hat{\lambda}_j \hat{a}_j^{\mathrm{CI}} + \hat{\mu}_j^{\mathrm{CI}} \hat{b}_j^{\mathrm{CI}}}{\hat{\lambda}_j^{\mathrm{CI}} + D_j^{\mathrm{CI}}} - \frac{1}{\hat{\Xi}_j^{\mathrm{CI}}}.$$

To solve the robust design problem in (60), similar steps as in Algorithm 1 are followed by adopting the corresponding CI based solutions as detailed in Section IV-B, respectively.

V. Simulation Results

In this section, we investigate the performance of our proposed schemes through Monte Carlo simulations. We consider the system with the FD BS at the centre of a cell with $N = 6$. We assume $K = 4$ DL users and $J = 2$ MDs, are randomly and uniformly distributed between the distance of 2m and 20m.

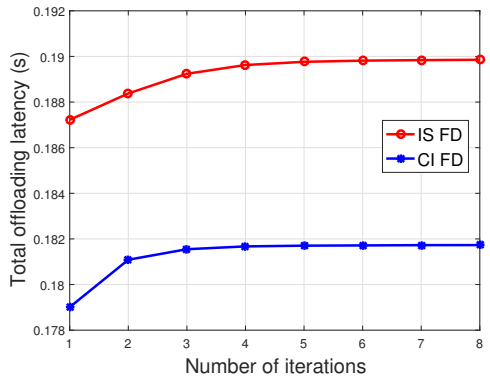

Fig. 3. Total offloading latency versus number of iterations.

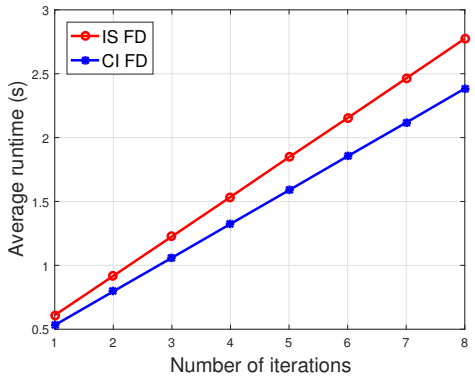

Fig. 4. Average Run time versus number of iterations.

We model the channels to the MDs and DL users as Rayleigh fading. The SI channel is modelled as Rician fading channel with Rician factor 6dB [6]. Furthermore, we consider a similar system set-up as in [5] with $\sigma_i = \sigma_j = -90$dB, $P_{\max}^{\mathrm{MD}} = 32$dBm and $P_{\max}^{\mathrm{DL}} = 40$dBm. Moreover, we assume $T = 100$ms, $\Gamma_i = 4$dB, $B = 1$MHz, $q_j = 10^5$, $L_{\mathrm{BS},j} = 10^3$ and $f_{\mathrm{BS}} = 10^{10}$ as in [12], [15], and QPSK modulation is considered for the CI scheme.

Our baseline is the HD scheme as in [18]. In order to make the comparison fair, we consider that the HD BS is equipped with N number of transmit and N number of receive antennas which are utilized for transmitting or receiving in non-overlapping equal-length time intervals. This implies that both self-interference (SI) and co-channel interference (CCI) are avoided. In addition, we set the data rate of HD equal to the one for FD, which requires that the individual mobile devices' and downlink users' data rates are double the ones for the FD case, due to the slotted HD transmission. Furthermore, the power consumption for the uplink and downlink transmission is divided by two since only uplink or downlink transmission is performed at a given time.

A. Convergence and Complexity of Algorithms

In this subsection, we show the convergence and complexity to the solutions for the proposed MOOPs in P(1) and P(2), respectively. Since the objective functions in P(1) and P(2) decrease in every iteration the convergence of Algorithm 1 is guaranteed, which can realized from optimizing all $\mathbf{w}_k$ and p_j in each iteration as shown in Algorithm 1. In Figs. 2 and 3, we show the convergence rate of the proposed solutions with respect to number of iterations. Each point in the curves is obtained by solving the MOOPs in P(1) and P(2) for the corresponding number of iteration(s). Generally, we have observed that both the proposed IS and CI schemes converge with the same number of iterations in terms of both the offloading energy and latency respectively, although, it takes fewer iterations for the case of the offloading latency. This is attributed to the strictness of the offloading latency threshold imposed for each mobile device. In addition, even with the same convergence rate, the CI scheme shows improved performance in both plots compared to the IS scheme since multi-user inference in exploited rather than suppressed. Furthermore, in Fig. 4, we show the corresponding complexity of the proposed solutions in terms of the average run time in seconds per iteration. We can observe that, although the solutions to proposed schemes have the same convergence rate, the average run time in seconds per iteration of the CI scheme is faster than the IS scheme. This difference in complexity mainly comes from optimizing the beamforming vectors $\mathbf{w}_k$ through solving subproblems (10) and (28) for the IS scheme and CI scheme, respectively. The formulation in (10) is a standard SDP problem which basically finds the optimal covariance matrix $\mathbf{W}_k$ before retrieving the beamforming vector $\mathbf{w}_k$, while (28) is a second-order cone program (SOCP) that finds the optimal beamforming vectors directly. In general, the solutions to the proposed MOOPs show an acceptable complexity as shown in Fig. 4.

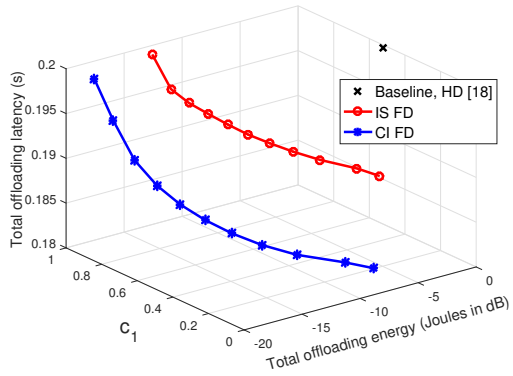

Fig. 5. Trade-off plot total offloading energy versus latency with $N = 6$, $K = 4$, $J = 2$, $T = 100$ms, $\Gamma_i = 4$dB, $B = 1$MHz, $q_j = 10^5$, $L_{\mathrm{BS},j} = 10^3$ and $f_{\mathrm{BS}} = 10^{10}$.

B. Numerical Results

Fig. 5 shows the trade-off between the total offloading energy and latency. The trade-off region is obtained by varying the weights c_1 and c_2 between 0 to 1, respectively, with a step size of 0.1. First, it can be seen that, where before one could only optimize either the offloading energy with a fixed latency constraint, or the latency with a fixed energy constraint, our proposed MOOP allows for a scalable tradeoff between the

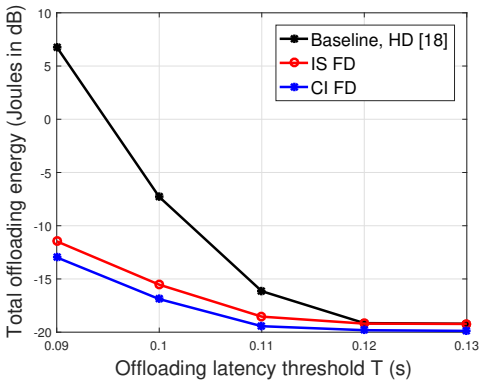

Fig. 6. Total offloading energy versus latency threshold T, with $N = 6$, $K = 4$, $J = 2$, $c_1 = c_2 = 0.5$, $\Gamma_i = 4$dB, $B = 1$MHz, $q_j = 10^5$, $L_{\mathrm{BS},j} = 10^3$ and $f_{\mathrm{BS}} = 10^{10}$.

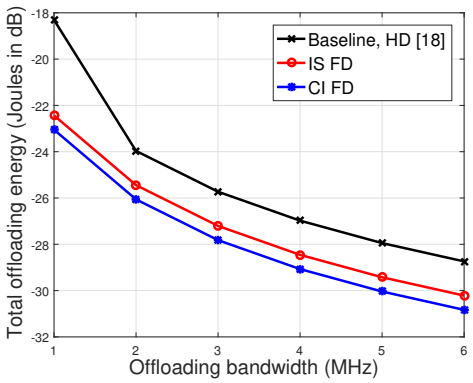

Fig. 8. Total offloading energy versus offloading bandwidth B, with $N = 6$, $K = 4$, $J = 2$, $c_1 = c_2 = 0.5$, $\Gamma_i = 4$dB, $T = 100$ms, $q_j = 10^5$, $L_{\mathrm{BS},j} = 10^3$ and $f_{\mathrm{BS}} = 10^{10}$.

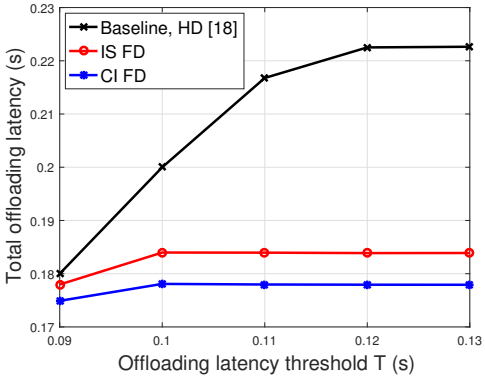

Fig. 7. Total offloading latency versus latency threshold T with $N = 6$, $K = 4$, $J = 2$, $c_1 = c_2 = 0.5$, $\Gamma_i = 4$dB, $B = 1$MHz, $q_j = 10^5$, $L_{\mathrm{BS},j} = 10^3$ and $f_{\mathrm{BS}} = 10^{10}$.

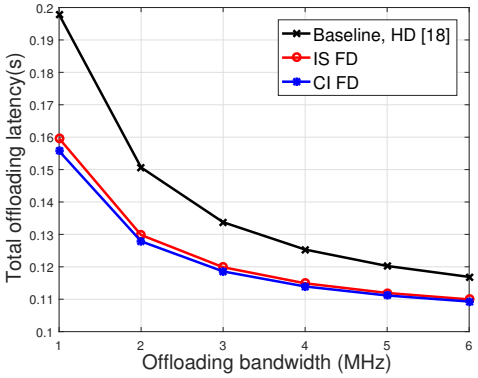

Fig. 9. Total offloading latency versus offloading bandwidth B, with $N = 6$, $K = 4$, $J = 2$, $c_1 = c_2 = 0.5$, $\Gamma_i = 4$dB, $T = 100$ms, $q_j = 10^5$, $L_{\mathrm{BS},j} = 10^3$ and $f_{\mathrm{BS}} = 10^{10}$.

two objectives. It is evident that an increase in the offloading energy leads to the decrease in the offloading latency and vice versa. This is as a result of the dependency of the optimization variables. On one hand, increasing the transmit power of the mobile devices in order to satisfy the latency constraints and minimize the offloading latency, increases the CCI to the downlink users. Hence, the downlink transmit power is increased to accommodate for the increase in CCI, which in turn increases the SI. In essence, this leads a continuous increase in the uplink and downlink transmit power, thus, the offloading energy increases. On the contrary, reducing the transmit powers in order to reduce the CCI and SI, and minimize the offloading energy, gives rise to an increase in the offloading latency. In addition, this results show the proposed CI scheme consumes less energy and time as compared to the conventional FD scheme. This is because less downlink transmit power is required to satisfy the downlink SINR constraints, hence, reduced SI, as compared to the conventional case where interference is rather suppressed. Furthermore, the points $c_1 = 0$ and $c_1 = 1$ is equivalent to the having only the offloading energy minimization problem [13], [15]–[17] and the offloading latency minimization problem [14], respectively. Again, this shows the flexibility provided by the proposed MOOP by varying the weights. More importantly, it can be seen that the proposed FD schemes out perform their baseline HD [18] counterpart in terms of energy consumption and latency reduction.

In Figs. 6 and 7, we study the effect of different offloading latency thresholds T on the considered system. Here, for the purpose of analyses we set $c_1 = c_2 = 0.5$. Fig. 6 shows the total offloading energy for the different latency thresholds. As expected for all the schemes, since increasing the latency threshold requires less transmit powers, thus, the total offloading energy consumption reduces, respectively. However, in terms of offloading latency in Fig. 7, all schemes are proportional to increase in latency requirement. Besides, in both plots the FD schemes outperforms the HD scheme. This further highlights the effectiveness of the proposed FD schemes.

Next, we show the effect of the offloading bandwidth (B) in the considered FD system. Fig. 8 shows that the total offloading energy consumption decreases as B increases. This indicates that as B increase the offloading rate increases and also energy consumption is saved by all schemes. However, still the proposed FD schemes outperforms the HD counterpart even at large bandwidth. Similar trend can be seen in Fig. 9,

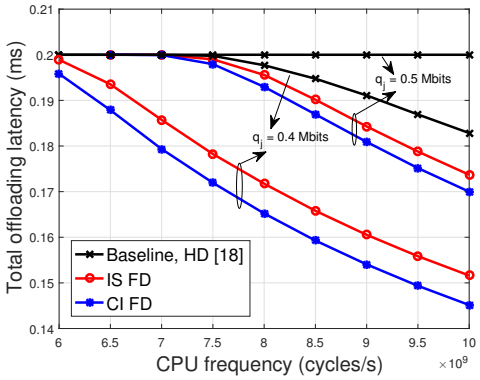

Fig. 10. Total offloading latency versus CPU frequency f_{BS}, with $N = 6, K = 4, J = 2, c_1 = c_2 = 0.5, \Gamma_i = 4$dB, $T = 100$ms, $B = 1$MHz and $L_{\text{BS},j} = 10^3$.

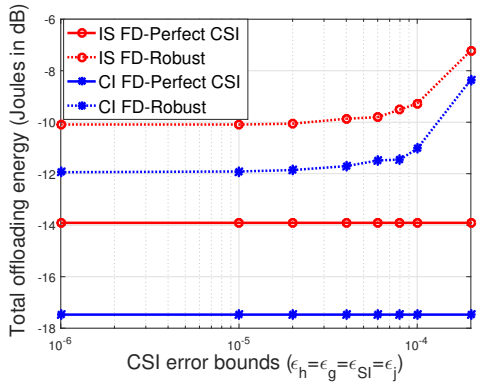

Fig. 11. Total offloading energy versus Error bounds ($\epsilon_h = \epsilon_g = \epsilon_{SI} = \epsilon_j$), with $N = 6, K = 4, J = 2, c_1 = c_2 = 0.5, \Gamma_i = 4$dB, $B = 1$MHz, $T = 100$ms, $q_j = 10^5$, $L_{\text{BS},j} = 10^3$ and $f_{\text{BS}} = 10^{10}$.

which shows that increasing B results in latency reduction. This is as a result of the increase in offloading rate which translates directly to reduction in latency. These plots highlight the importance of the offloading bandwidth in the considered FD system.

In addition, Fig. 10 shows the total offloading latency versus the CPU frequency of the FD BS. As the CPU frequency increases, less time is required by the FD BS to complete the computation of the offloaded tasks. This is reported in Fig. 10 for all schemes. The figure also shows the effect of the computation task size with regards to the CPU frequency. It can be seen that an increase in the computation task size increases the overall offloading latency. This is obviously due the fact that increasing the task size implies more cycles/s is required to complete the task, hence, an increase in the overall latency. Besides, our proposed FD schemes outperform the HD scheme in all cases.

Furthermore, in Figs. 11 and 12 we investigate the performance of the proposed robust FD schemes. Fig. 11 shows the obtained total energy consumption with increasing CSI error bounds where it can be seen that increasing error bound increases the energy consumption. The reason is that increasing the error bounds implies reduced CSI knowledge at the FD BS. Similarly, in Fig. 12, the total latency increases

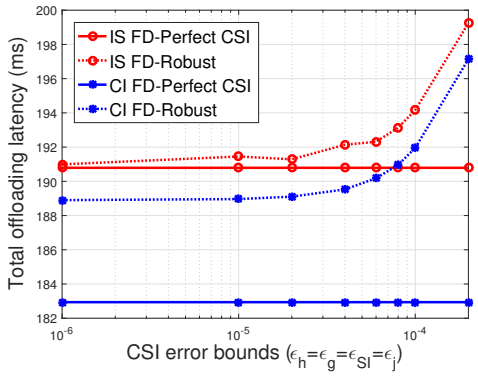

Fig. 12. Total offloading latency versus Error bounds ($\epsilon_h = \epsilon_g = \epsilon_{SI} = \epsilon_j$), with $N = 6, K = 4, J = 2, c_1 = c_2 = 0.5, \Gamma_i = 4$dB, $B = 1$MHz, $T = 100$ms, $q_j = 10^5$, $L_{\text{BS},j} = 10^3$ and $f_{\text{BS}} = 10^{10}$.

with increase in the CSI error bounds.

VI. Conclusion

In this paper, we studied the offloading energy and latency trade-off in a multiuser FD system that performs both data transmission and MEC. We proposed one FD scheme based on the traditional downlink MUI interference suppression and the other based on downlink MUI exploitation. We further extended the two proposed schemes to consider practical scenarios with imperfect CSI knowledge. The proposed FD schemes show a promising performance improvement over the baseline HD schemes.

References

[1] D. Bharadia, E. McMilin, and S. Katti, "Full duplex radios," in *ACM SIGCOMM Computer Communication Review*, vol. 43, no. 4. ACM, 2013, pp. 375–386.

[2] M. Duarte, A. Sabharwal, V. Aggarwal, R. Jana, K. Ramakrishnan, C. W. Rice, and N. Shankaranarayanan, "Design and characterization of a full-duplex multiantenna system for WiFi networks," *IEEE Transactions on Vehicular Technology*, vol. 63, no. 3, pp. 1160–1177, 2014.

[3] H. Q. Ngo, H. A. Suraweera, M. Matthaiou, and E. G. Larsson, "Multipair full-duplex relaying with massive arrays and linear processing," *IEEE Journal on Selected Areas in Communications*, vol. 32, no. 9, pp. 1721–1737, 2014.

[4] D. W. K. Ng, Y. Wu, and R. Schober, "Power efficient resource allocation for full-duplex radio distributed antenna networks," *IEEE Transactions on Wireless Communications*, vol. 15, no. 4, pp. 2896–2911, 2016.

[5] Y. Sun, D. W. K. Ng, J. Zhu, and R. Schober, "Multi-objective optimization for robust power efficient and secure full-duplex wireless communication systems," *IEEE Transactions on Wireless Communications*, vol. 15, no. 8, pp. 5511–5526, 2016.

[6] S. Leng, D. W. K. Ng, N. Zlatanov, and R. Schober, "Multi-objective resource allocation in full-duplex SWIPT systems," in *Communications (ICC), 2016 IEEE International Conference on*. IEEE, 2016, pp. 1–7.

[7] H. A. Suraweera, I. Krikidis, G. Zheng, C. Yuen, and P. J. Smith, "Low-complexity end-to-end performance optimization in mimo full-duplex relay systems." *IEEE Trans. Wireless Communications*, vol. 13, no. 2, pp. 913–927, 2014.

[8] E. Sharma, R. Budhiraja, K. Vasudevan, and L. Hanzo, "Full-duplex massive mimo multi-pair two-way af relaying: Energy efficiency optimization," *IEEE Transactions on Communications*, 2018.

[9] M. T. Kabir, M. R. A. Khandaker, and C. Masouros, "Reducing self-interference in full duplex transmission by interference exploitation," *IEEE Global Communications Conference*, pp. 1–6, Dec 2017.

[10] M. T. Kabir, M. R. Khandaker, and C. Masouros, "Robust energy harvesting FD transmission: Interference suppression vs exploitation," *IEEE Communications Letters*, vol. 22, no. 9, pp. 1866–1869, 2018.

[11] ——, "Interference exploitation in full-duplex communications: Trading interference power for both uplink and downlink power savings," *IEEE Transactions on Wireless Communications*, vol. 17, no. 12, pp. 8314–8329, 2018.

[12] S. Barbarossa, S. Sardellitti, and P. Di Lorenzo, "Communicating while computing: Distributed mobile cloud computing over 5G heterogeneous networks," *IEEE Signal Processing Magazine*, vol. 31, no. 6, pp. 45–55, 2014.

[13] C. You, K. Huang, H. Chae, and B.-H. Kim, "Energy-efficient resource allocation for mobile-edge computation offloading," *IEEE Transactions on Wireless Communications*, vol. 16, no. 3, pp. 1397–1411, 2017.

[14] L. Yang, J. Cao, H. Cheng, and Y. Ji, "Multi-user computation partitioning for latency sensitive mobile cloud applications," *IEEE Transactions on Computers*, vol. 64, no. 8, pp. 2253–2266, 2015.

[15] F. Wang, J. Xu, X. Wang, and S. Cui, "Joint offloading and computing optimization in wireless powered mobile-edge computing systems," *IEEE Transactions on Wireless Communications*, vol. 17, no. 3, pp. 1784–1797, 2018.

[16] S. Sardellitti, G. Scutari, and S. Barbarossa, "Joint optimization of radio and computational resources for multicell mobile-edge computing," *IEEE Transactions on Signal and Information Processing over Networks*, vol. 1, no. 2, pp. 89–103, 2015.

[17] X. Chen, L. Jiao, W. Li, and X. Fu, "Efficient multi-user computation offloading for mobile-edge cloud computing," *IEEE/ACM Transactions on Networking*, no. 5, pp. 2795–2808, 2016.

[18] T. Q. Dinh, J. Tang, Q. D. La, and T. Q. Quek, "Offloading in mobile edge computing: Task allocation and computational frequency scaling," *IEEE Transactions on Communications*, vol. 65, no. 8, pp. 3571–3584, 2017.

[19] Z. Wen, K. Yang, X. Liu, S. Li, and J. Zou, "Joint offloading and computing design in wireless powered mobile-edge computing systems with full-duplex relaying," *IEEE Access*, vol. 6, pp. 72 786–72 795, 2018.

[20] S. Mao, S. Leng, K. Yang, X. Huang, and Q. Zhao, "Fair energy-efficient scheduling in wireless powered full-duplex mobile-edge computing systems," in *GLOBECOM 2017-2017 IEEE Global Communications Conference*. IEEE, 2017, pp. 1–6.

[21] Z. Tan, F. R. Yu, X. Li, H. Ji, and V. C. Leung, "Virtual resource allocation for heterogeneous services in full duplex-enabled scns with mobile edge computing and caching," *IEEE Transactions on Vehicular Technology*, vol. 67, no. 2, pp. 1794–1808, 2018.

[22] M. Liu, Y. Mao, S. Leng, and S. Mao, "Full-duplex aided user virtualization for mobile edge computing in 5g networks," *IEEE Access*, vol. 6, pp. 2996–3007, 2018.

[23] X. Ge, S. Tu, G. Mao, C.-X. Wang, and T. Han, "5g ultra-dense cellular networks," *IEEE Wireless Communications*, vol. 23, no. 1, pp. 72–79, 2016.

[24] B. Li, H. H. Dam, A. Cantoni, and K. L. Teo, "Some interesting properties for zero-forcing beamforming under per-antenna power constraints in rural areas," *Journal of Global Optimization*, vol. 62, no. 4, pp. 877–886, 2015.

[25] B. P. Day, A. R. Margetts, D. W. Bliss, and P. Schniter, "Full-duplex mimo relaying: Achievable rates under limited dynamic range," *IEEE Journal on Selected Areas in Communications*, vol. 30, no. 8, pp. 1541–1553, 2012.

[26] Y. Mao, C. You, J. Zhang, K. Huang, and K. B. Letaief, "A survey on mobile edge computing: The communication perspective," *IEEE Communications Surveys & Tutorials*, vol. 19, no. 4, pp. 2322–2358, 2017.

[27] R. T. Marler and J. S. Arora, "Survey of multi-objective optimization methods for engineering," *Structural and multidisciplinary optimization*, vol. 26, no. 6, pp. 369–395, 2004.

[28] Z.-Q. Luo, W.-K. Ma, A. M.-C. So, Y. Ye, and S. Zhang, "Semidefinite relaxation of quadratic optimization problems," *IEEE Signal Processing Magazine*, vol. 27, no. 3, pp. 20–34, 2010.

[29] C. Masouros, T. Ratnarajah, M. Sellathurai, C. B. Papadias, and A. K. Shukla, "Known interference in the cellular downlink: A performance limiting factor or a source of green signal power?" *IEEE Communications Magazine*, vol. 51, no. 10, pp. 162–171, 2013.

[30] C. Masouros, M. Sellathurai, and T. Ratnarajah, "Vector perturbation based on symbol scaling for limited feedback miso downlinks," *IEEE Transactions on Signal Processing*, vol. 62, no. 3, pp. 562–571, 2014.

[31] P. V. Amadori and C. Masouros, "Constant envelope precoding by interference exploitation in phase shift keying-modulated multiuser transmission," *IEEE Transactions on Wireless Communications*, vol. 16, no. 1, pp. 538–550, 2017.

[32] C. Masouros and G. Zheng, "Exploiting known interference as green signal power for downlink beamforming optimization," *IEEE Transactions on Signal processing*, vol. 63, no. 14, pp. 3628–3640, 2015.

[33] P. V. Amadori and C. Masouros, "Large scale antenna selection and precoding for interference exploitation," *IEEE Transactions on Communications*, vol. 65, no. 10, pp. 4529–4542, 2017.

[34] A. Li and C. Masouros, "Exploiting constructive mutual coupling in p2p mimo by analog-digital phase alignment," *IEEE Transactions on Wireless Communications*, vol. 16, no. 3, pp. 1948–1962, 2017.

[35] S. Timotheou, G. Zheng, C. Masouros, and I. Krikidis, "Exploiting constructive interference for simultaneous wireless information and power transfer in multiuser downlink systems," *IEEE Journal on Selected Areas in Communications*, vol. 34, no. 5, pp. 1772–1784, 2016.

[36] K. L. Law and C. Masouros, "Detection region based beamforming for interference exploitation," *IEEE Transaction on Communications*, in press.

[37] A. Li and C. Masouros, "Interference exploitation precoding made practical: Optimal closed-form solutions for PSK modulations," *IEEE Transaction on Wireless Communications*, in press.

[38] A. Li, C. Masouros, F. Liu, and L. Swindlehurst, "Massive MIMO 1-Bit DAC transmission: A low-complexity symbol scaling approach," *IEEE Transaction on Wireless Communications*, in press.

[39] N. Vucic and H. Boche, "Robust qos-constrained optimization of downlink multiuser miso systems," *IEEE Transactions on Signal Processing*, vol. 57, no. 2, pp. 714–725, 2009.

[40] S. Boyd and L. Vandenberghe, *Convex optimization*. Cambridge university press, 2004.

Mahmoud T. Kabir (S'17) received his Bachelor's degree in Electrical and Electronic Engineering from University of Sussex, UK, in 2012 and his Master's degree in Communication Engineering from University of Manchester, UK, in 2013. He is currently working towards the Ph.D. degree in the Communications and Information Systems Research Group, Department of Electrical and Electronic Engineering, University College London, UK. His research interests include precoding designs for MIMO systems, full-duplex systems and convex optimization.

Christos Masouros (SMIEEE, MIET) received the Diploma degree in Electrical and Computer Engineering from the University of Patras, Greece, in 2004, and MSc by research and PhD in Electrical and Electronic Engineering from the University of Manchester, UK in 2006 and 2009 respectively. In 2008 he was a research intern at Philips Research Labs, UK. Between 2009-2010 he was a Research Associate in the University of Manchester and between 2010-2012 a Research Fellow in Queen's University Belfast. In 2012 he joined University College London as a Lecturer. He has held a Royal Academy of Engineering Research Fellowship between 2011-2016.

He is currently an Associate Professor in the Communications and Information Systems research group, Dept. Electrical and Electronic Engineering, University College London. His research interests lie in the field of wireless communications and signal processing with particular focus on Green Communications, Large Scale Antenna Systems, Cognitive Radio, interference mitigation techniques for MIMO and multicarrier communications. He was the recipient of the Best Paper Award in the IEEE GlobeCom 2015 conference, and has been recognised as an Exemplary Editor for the IEEE Communications Letters, and as an Exemplary Reviewer for the IEEE Transactions on Communications. He is an Editor for IEEE Transactions on Communications, an Associate Editor for IEEE Communications Letters, and was a Guest Editor for IEEE Journal on Selected Topics in Signal Processing issues "Exploiting Interference towards Energy Efficient and Secure Wireless Communications" and "Hybrid Analog / Digital Signal Processing for Hardware-Efficient Large Scale Antenna Arrays". He is currently an elected member of the EURASIP SAT Committee on Signal Processing for Communications and Networking.